Global Ozone Observations from the *UARS* MLS: An Overview of Zonal-Mean Results

LUCIEN FROIDEVAUX, JOE W. WATERS, WILLIAM G. READ, LEE S. ELSON, DENNIS A. FLOWER, AND ROBERT F. JARNOT

Jet Propulsion Laboratory, California Institute of Technology, Pasadena, California

(Manuscript received 22 March 1994, in final form 21 June 1994)

ABSTRACT

Global ozone observations from the Microwave Limb Sounder (MLS) aboard the *Upper Atmosphere Research Satellite (UARS)* are presented, in both vertically resolved and column abundance formats. The authors review the zonal-mean ozone variations measured over the two and a half years since launch in September 1991. Well-known features such as the annual and semiannual variations are ubiquitous. In the equatorial regions, longer-term changes are believed to be related to the quasi-biennial oscillation (QBO), with a strong semiannual signal above 20 hPa. Ozone values near 50 hPa exhibit an equatorial low from October 1991 to June 1992, after which the low ozone pattern splits into two subtropical lows (possibly in connection with residual circulation changes tied to the QBO) and returns to an equatorial low in September 1993. The ozone hole development at high southern latitudes is apparent in MLS column data integrated down to 100 hPa, with a pattern generally consistent with *Nimbus-7* Total Ozone Mapping Spectrometer (TOMS) measurements of total column; the MLS data reinforce current knowledge of this lower-stratospheric phenomenon by providing a height-dependent view of the variations. The region from 30°S to 30°N (an area equal to half the global area) shows very little change in the ozone column from year to year and within each year.

The most striking ozone changes have occurred at northern midlatitudes, with the October 1992 to July 1993 column values significantly lower than during the prior year. The zonal-mean changes manifest themselves as a slower rate of increase during the 1992/93 winter, and there is some evidence for a lower fall minimum. A recovery occurs during late summer of 1993; early 1994 values are significantly larger than during the two previous winters. These results are in general agreement with variations measured by the *Nimbus-7* TOMS and *Meteor-3* TOMS instruments at midlatitudes. However, the southern midlatitudes exhibit less of a column ozone decrease (relative to the north) in the MLS data (down to 100 hPa) than in the TOMS column results. The timing and latitudinal extent of the northern midlatitude decreases appear to rule out observed ClO enhancements in the Arctic vortex, with related chemical processing and ozone dilution effects, as a unique cause. Local depletion from ClO-related chemical mechanisms alone is also not sufficient, based on MLS ClO data. The puzzling asymmetric nature of the changes probably requires a dynamical component as an explanation. A combination of effects (including chemical destruction via heterogeneous processes and QBO phasing) apparently needs to be invoked. This dataset will place constraints on future modeling studies, which are required to better understand the source of the observed changes.

Finally, residual ozone values extracted from TOMS-minus-MLS column data are briefly presented as a preliminary view into the potential usefulness of such studies, with information on tropospheric ozone as an ultimate goal.

1. Introduction

There have been various reports of stronger than expected declines in ozone during the last two years, from satellite measurements (Gleason et al. 1993; Herman and Larko 1994; Planet et al. 1994) to ground-based and balloon-based data (Grant et al. 1992, 1994; Kerr et al. 1993; Bojkov et al. 1993; Hofmann et al. 1993, 1994; Komhyr et al. 1994). The potential for ozone destruction as a result of heterogeneous reactions occurring on volcanic (sulphate) aerosols has been increasingly discussed since the large eruption of the El Chichón volcano in 1982 and its possible relation to ozone changes (Hofmann and Solomon 1989). The possible impact of the June 1991 eruption of Mount Pinatubo on ozone is a subject of much current interest, given the large increase in stratospheric volcanic aerosol from that eruption (Bluth et al. 1992; McCormick and Veiga 1992; McCormick et al. 1994).

The *Upper Atmosphere Research Satellite (UARS)* was launched on 12 September 1991, with 10 instruments of international origin aboard (Reber 1993). The study of upper-atmospheric chemistry and dynamics, coupled with *UARS* measurements of solar flux and

Corresponding author address: Dr. Lucien Froidevaux, Mail Stop 183-701, Jet Propulsion Laboratory, 4800 Oak Grove Drive, Pasadena, CA 91109.

energetic particles, is at the center of this mission's research goals.

Ozone measurements from the Microwave Limb Sounder (MLS) are described in this paper, for the period between October 1991 and March 1994. We focus on the zonal-mean variations observed throughout the globe during this interesting time. This overview is meant to present some of the more obvious features seen in MLS data, even though a full interpretation (with model comparisons) will have to await further studies. Since the MLS data are now being released to the non-*UARS* community, it is hoped that this paper can guide other interested scientists toward certain areas of research in relation to this dataset. Elson et al. (1994) give an overview of the large-scale wave components observed in the MLS ozone data. Some words of caution and caveats are given in section 2 regarding retrieval uncertainties and known systematics, even though a product of good quality overall has been achieved so far. The dataset presented here was generated from MLS Version 3/level 3AL data files on the Central Data Handling Facility at the Goddard Space Flight Center; these files are being stored on the Distributed Active Archive Center (DAAC), also at Goddard. Further details and profile intercomparisons with other datasets will be given in upcoming publications. In section 3, zonal-mean ozone mixing ratios at various latitudes from 80°S to 80°N are presented; some emphasis is placed on changes observed at low latitudes and the possible connection with the QBO. The ozone abundances are then integrated in the vertical to produce zonal-mean column measurements for various pressure intervals; this is discussed primarily in section 4. We focus in section 5 on the ozone column behavior at midlatitudes (30°–60° bin) and the significant differences observed during the first two years of MLS operation, along with possible explanations for these measurements. Comparisons with both the *Nimbus-7* and *Meteor-3* Total Ozone Mapping Spectrometer (TOMS) ozone column data are made. Section 6 gives a brief presentation of residual ozone column obtained from a subtraction of MLS column from TOMS total column data as a topic worthy of further study, regarding the possibility of extracting variations in tropospheric ozone.

2. MLS ozone retrievals

The MLS instrument measures thermal emission at millimeter wavelengths by scanning through the atmospheric limb (Waters 1993). An instrument description has been given by Barath et al. (1993), and first results on polar ClO and ozone in the lower stratosphere are described in Waters et al. (1993a). Temperature (with tangent pressure registration from O_2 lines at 63 GHz) and water vapor (e.g., Harwood et al. 1993) are the other primary products, and retrievals of SO_2 (Read et al. 1993) and, more recently, HNO_3 have also been performed. Ozone is measured in two distinct spectral bands by the 205-GHz and 183-GHz radiometers, and independent retrievals are carried out for each band. We report here on the 205-GHz results only, because they have shown somewhat better accuracy than the 183-GHz results and because they cover a longer time period (the 183-GHz radiometer measuring H_2O and O_3 stopped operating in mid-April 1993). Stratospheric abundances and variations are emphasized here (mesospheric information is mostly obtainable from the 183-GHz ozone retrievals). Atmospheric profiles retrieved in this fashion are spaced about 4 degrees apart in latitude, with better coverage near the latitudes corresponding to orbit turnaround. These turnaround points occur at about 34°N (34°S) and 80°S (80°N) when the satellite is flying forward (backward), with the alternating coverage arising as a result of the *UARS* yaw maneuvers (roughly every 36 days), tied to the orbit precession. There are 15 orbits per day, so that each latitude (at the 4° resolution) is sampled about 30 times during a 24-h period. This type of sampling goes into the zonal means discussed throughout this paper.

Substantial details on MLS ozone retrievals and comparisons with other datasets will be discussed in upcoming work, and continued validation and refinements in the retrievals are to be expected.

The MLS retrieval technique uses a sequential estimation approach (Rodgers 1976) to obtain tangent pressure and temperature from the 63-GHz band, followed by mixing ratio retrievals in the other bands. Climatological a priori profiles, provided by *UARS* investigators (based on existing datasets, and models where data are lacking), are combined with the data in this technique, mostly for stability in altitude regions where measurement sensitivity is rapidly degrading; we have used large a priori errors to ensure that minimal bias is introduced in the retrievals. Given the linearity in the radiative transfer at these wavelengths, a single-pass fit gives good results, and we have not used optically thick channels. However, further improvements can be expected with a fully iterative retrieval, to be implemented for the next major reprocessing of the MLS data. The current retrieval mixing ratio profiles consist of joined linear segments having three equally spaced breakpoints per decade change in $\log p$ (i.e., at pressures of 100, 46, 22 hPa, . . .), which corresponds to a vertical (level 2) grid with roughly 6-km spacing. The atmospheric profiles are retrieved as the breakpoint values. An approximate interpretation of these values, relative to the true (infinite resolution) profile, is the least-squares fit of the linearly segmented retrieval profile to the true one. The integrated column is essentially conserved regardless of the retrieval grid spacing. The level 3 standard *UARS* grid is twice as fine as the MLS level 2 grid—that is, it has six points per decade in $\log p$ rather than three. The MLS values at the nonretrieved level 3 grid points are averages of the level 2

coefficient values on either side. A trade-off exists between vertical resolution and profile noise; the optimum MLS vertical resolution is 5 points per decade in log$p$, which is only slightly coarser than the level 3 grid spacing. Profiles retrieved from MLS observations should generally be sensitive to features with vertical scale of a few kilometers. Smearing effects from the antenna field of view and radiative transfer through the atmosphere lead to a vertical smearing of 3.2 km (4 km is often quoted as vertical resolution). Current estimates of retrieval precision ("one sigma noise estimate") for single profiles are 0.3 ppmv (parts per million by volume) between 1 and 4.6 hPa, 0.2 ppmv between 10 and 46 hPa, and 0.5 ppmv at 100 hPa; these values correspond to roughly 1%–2% random errors at the ozone peak near 10 hPa, 5%–10% errors in the upper stratosphere, and large percentage errors near 100 hPa, where the mixing ratios are small and historically difficult to measure accurately on a global scale. These figures are based on observed summertime variability (rms deviation about the mean) in latitude bands near turnaround (30°–35°N or 30°–35°S), where a large number of profiles can be obtained in a narrow latitude range, as well as in the relatively quiet tropical regions (5°S–5°N); true precision may be slightly better than the minimum standard deviation obtained for the eight days used in this analysis, but theoretical estimates agree well with this empirical method of estimating precision. For zonal means in a typical 5°-wide latitude bin, with about 40–45 individual measurements included, precision is expected to be of order 0.1 ppmv or less. In terms of the noise component on column ozone calculated by integrating the retrieved profiles in the vertical, as done in this paper, the correlation between levels leads to some cancellation of errors. Our estimates of column precision, using the minimum observed variability in "quiet" periods/locations and near turnaround points (from a sample of eight days, each with over 100 profiles in two separate latitude bins) are 7, 2, and 1 DU (Dobson units) for column ozone calculated above 100, 46, and 22 hPa, respectively. For zonal means in a typical 5°-wide bin, these column precision estimates will go down by a factor of about 6.

However, systematic errors will not "average out." Based on comparisons with other datasets, and based on examination of the fields themselves, we find that there are small biases at certain pressure levels. In particular, the 46-hPa MLS values may be somewhat low (a few tenths of a ppmv), whereas the 100-hPa values show an opposite bias (of order 0.1–0.2 ppmv high). The retrieval technique relies on fitting the spectral contrast within the instrument bandpass. In the lowermost stratosphere, this contrast is significantly reduced in comparison with the middle to upper stratosphere, and it becomes difficult to separate from contributions (some better taken into account than others) from HNO_3, H_2O, N_2O, dry air continuum, and other small instrumental or computational effects. It is expected that updated retrieval software will produce improvements in ozone (205-GHz band), thanks in part to simultaneous retrievals of HNO_3, which can lead to changes in O_3 of order a few tenths of a ppmv in the lower stratosphere. We sometimes get zonal-mean values that are negative at 100 hPa (the lowest level for reasonable MLS sensitivity), particularly in the summer months at tropical latitudes; this bias is not yet removed or completely understood. Finally, small oscillations in the mean field, tied to the *UARS* "yaw cycle"—36-day variation—are known to exist (see figures later in the paper), particularly in the lowermost stratosphere; small discontinuities can also appear when a yaw day is crossed. These features may be propagated to ozone through the retrieved tangent pressures, and further investigation is necessary to fully understand and remove these effects, which are present at the few percent level.

The above issues should not affect the main results presented here, which mostly deal with zonal-mean trends. For example, excellent tracking has been obtained between MLS and Stratospheric Aerosol and Gas Experiment (SAGE) II ozone-mean values (D. Cunnold 1993, personal communication), despite a small offset between the two datasets (5%–10% higher values seen in MLS ozone), and other high-quality comparisons with ground-based, ozonesonde data and other *UARS* instruments have been made (to be published later). The MLS zonal-mean radiances are generally fit by "forward model" radiances (using retrieved MLS fields) to within about one percent (rms).

We now turn to a description of some of the interesting aspects of these 2.5 years of MLS data on zonal-mean ozone.

3. Ozone mixing ratio data

Figure 1 is a time series representation of zonal-mean ozone volume mixing ratio for four pressure levels (46, 22, 10, and 2 hPa), from October 1991 to March 1994. These zonal means are computed from MLS level 3AL data (stored every 4° of latitude). Because of the *UARS* cyclic "yaw maneuver," MLS observations alternate between mostly northern and mostly southern latitudes (coverage from 34°S to 80°N, followed by 34°N to 80°S). This leads to roughly 36-day gaps in MLS data at latitudes poleward of 34°N or 34°S (see Fig. 1). Other gaps occasionally occur because of missing or bad data caused by problems with the instrument or satellite. Figure 1 is useful for identifying changes from one year to the next. Figures 2 and 3 also display zonal-mean MLS ozone mixing ratio data (for all retrieval points between 100 and 2.2 hPa, i.e., at 100, 46, 22, 10, 5, and 2 hPa), but as color contour plots. This displays certain variations more effectively than in Fig. 1.

There are a number of general points that one can make based on the above figures. For example, largest

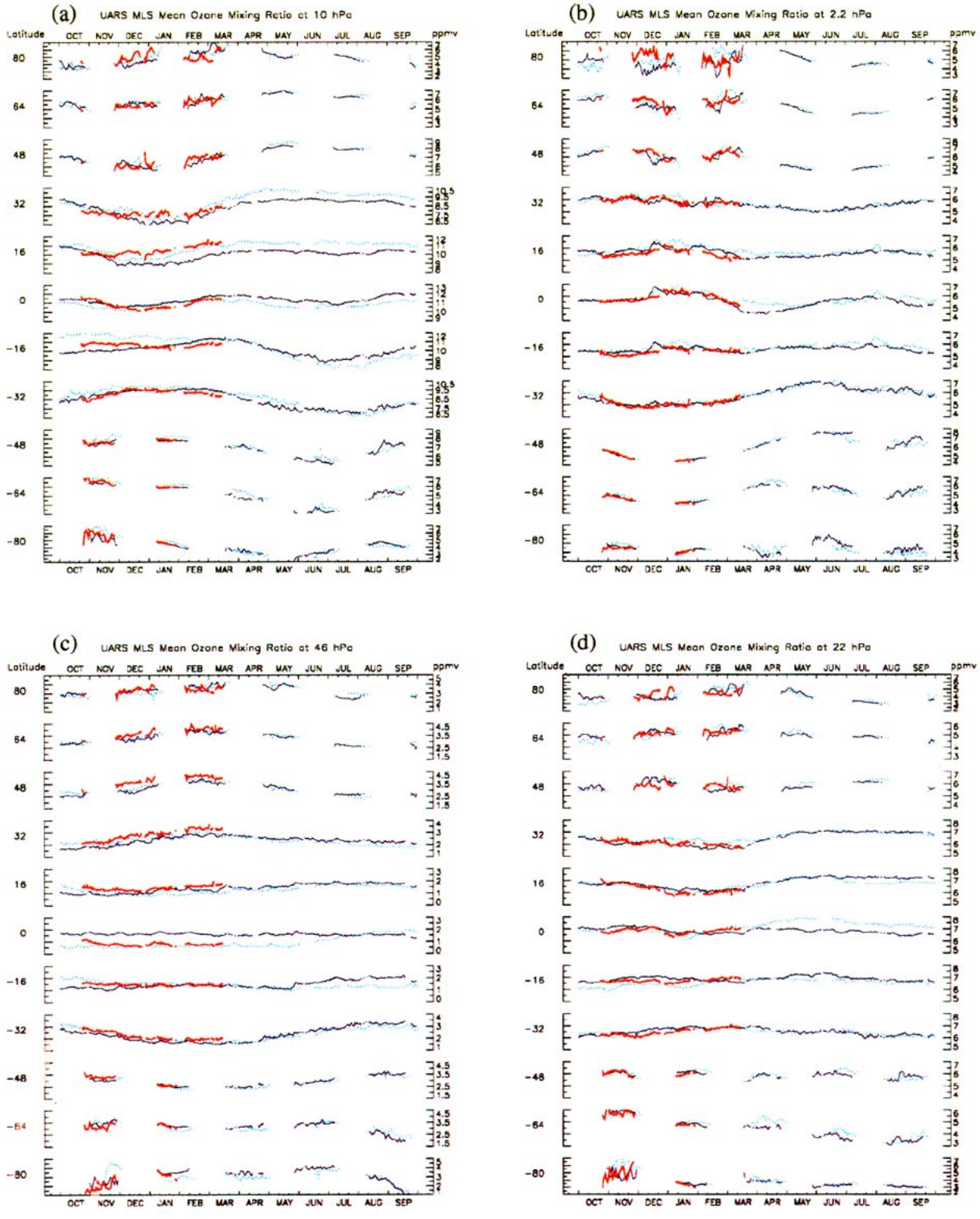

FIG. 1. Zonal-mean ozone volume mixing ratio time series for 1 October 1991 through 14 March 1994, from 80°S to 80°N (in 16° increments), based on MLS (level 3AL) data. Retrievals for four different retrieval pressures are shown: (a) 10 hPa, (b) 2 hPa, (c) 46 hPa, and (d) 22 hPa. October 1991 through September 1992 values are given by the light-blue dotted line, the following year is given by the dark-blue solid line, and the October 1993 through mid-March 1994 period is shown by the red solid line. Gaps in the time series occur at middle to high latitudes because of the alternating coverage between north and south (see text).

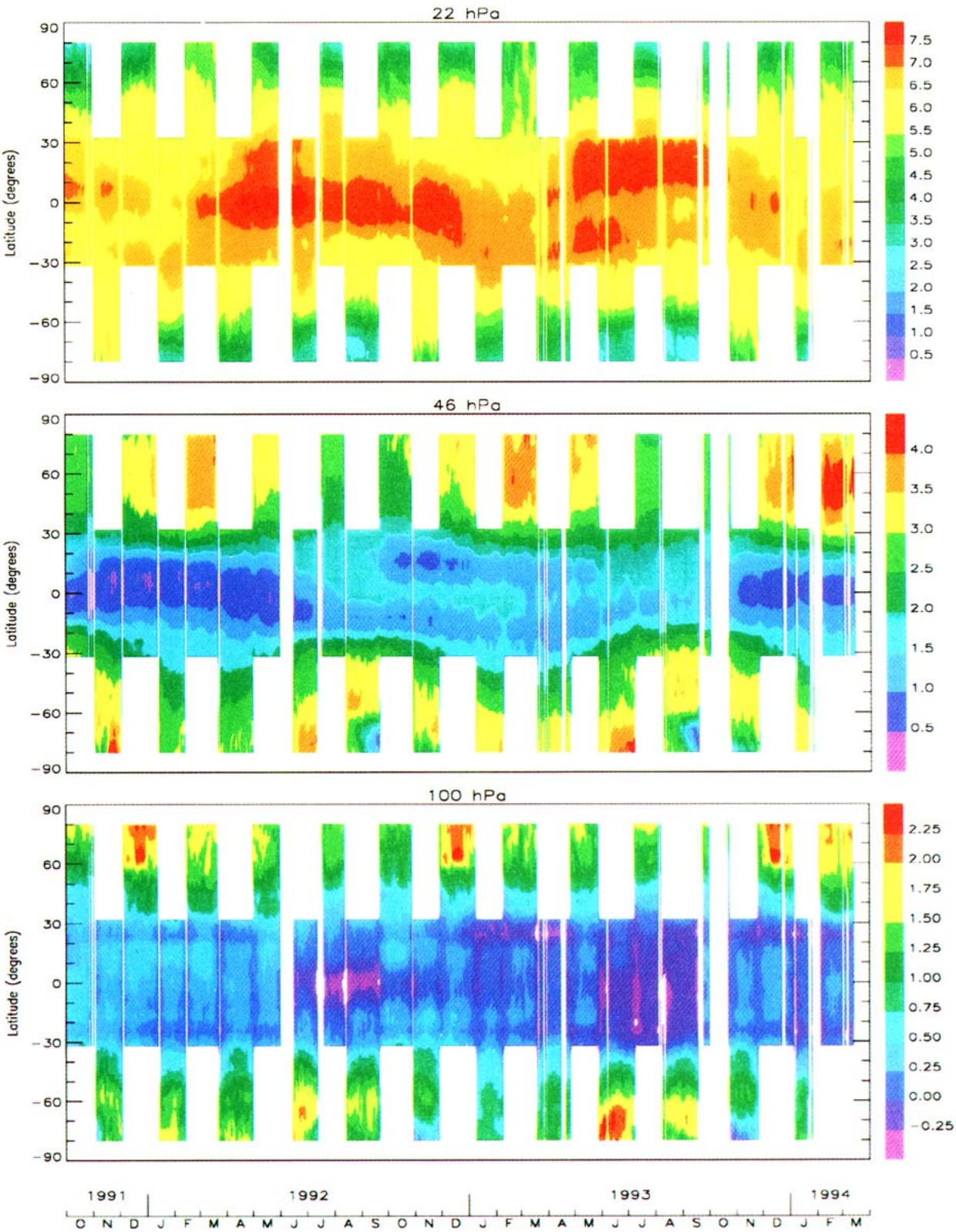

FIG. 2. Stratospheric zonal-mean ozone mixing ratios (ppmv), based on MLS (level 3AL) data. Contour plots are shown as a function of latitude and time, for 1 October 1991–14 March 1994. Panels are labeled with the surface pressure of the retrieved field (22, 46, and 100 hPa from top to bottom).

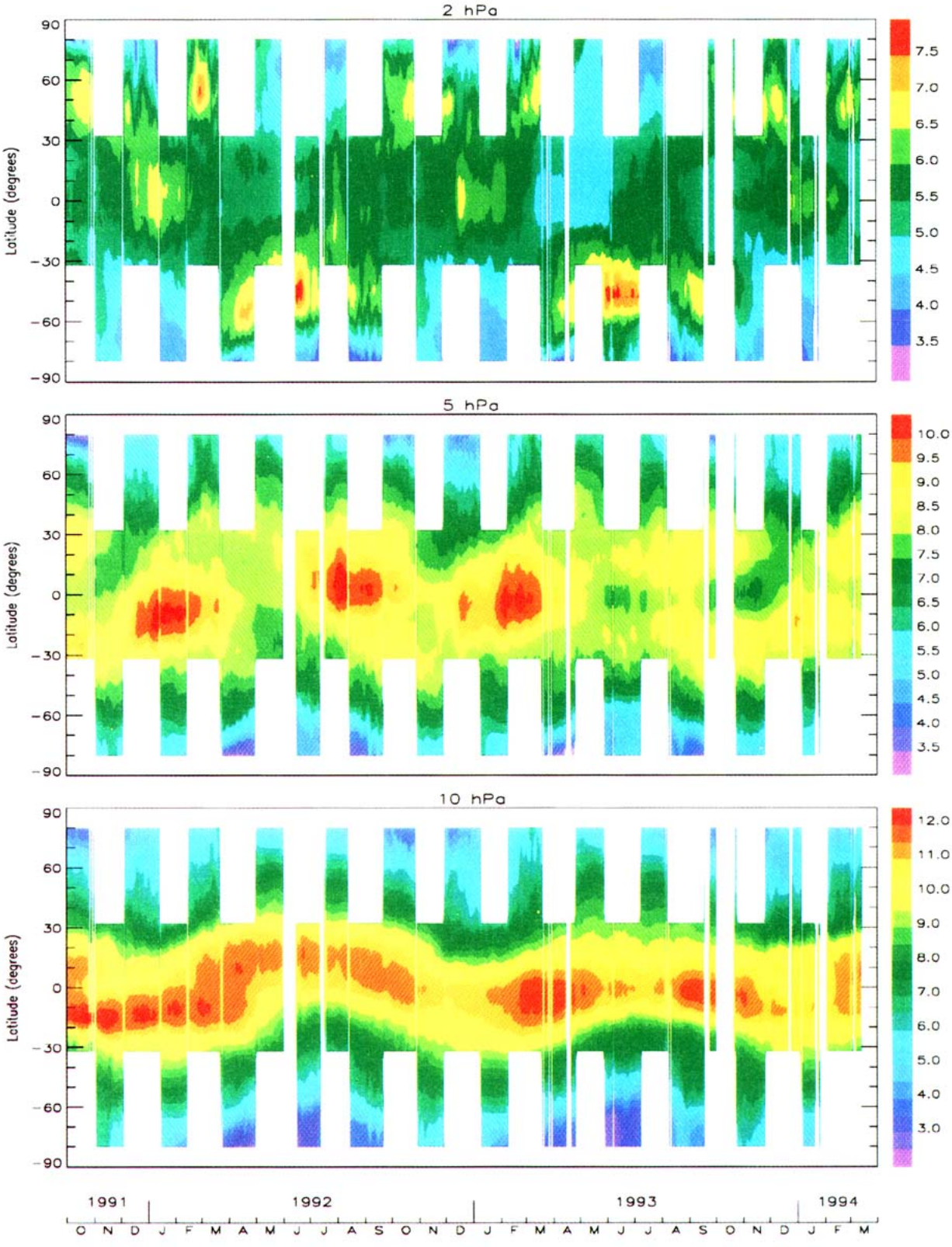

FIG. 3. Same as Fig. 2 but for 2 (i.e., 2.2), 5 (i.e., 4.6), and 10 hPa, from top to bottom.

ozone mixing ratios are observed at equatorial latitudes in the midstratosphere (see the 10-hPa plots), and largest variability is observed at high latitudes in winter, as expected. Note that small temporal oscillations can be seen (probably best in Figs. 2 and 3 in the Tropics), tied to the *UARS* yaw period of approximately 36 days. These are known artifacts in MLS data, and investigations continue regarding these effects, which are present at the few percent level. The lower-stratospheric ozone maxima are observed during February and March in the Northern Hemisphere middle to high latitudes, with a similar peak during August and September in the Southern Hemisphere (see the 46-hPa plots); this spring maximum is caused by transport of high-ozone air from the Tropics, where the primary production occurs, with a subsequent decrease induced by increasing photochemical destruction (e.g., Perliski et al. 1989). The ozone hole–related decrease in ozone during August and September is observed at the highest southern latitudes, in the lower stratosphere; a synoptic view of early results from MLS in the 1992 winter over these regions was given by Waters et al. (1993b). We will come back to the ozone hole briefly in section 4, but the polar regions are not the main emphasis of this paper; see Manney et al. (1994a,b) for recent discussions of polar ozone loss based on *UARS* data from MLS and the Cryogenic Limb Array Etalon Spectrometer (CLAES).

In the midstratosphere (see the 10-hPa plots) at middle to high latitudes, the annual cycle dominates as a consequence of significant photochemical production, which maximizes in the summer. This annual variation is observed, with the expected 6-month shift between hemispheres. A well-known semiannual oscillation (SAO) dominates at low latitudes in the middle to upper stratosphere, as observed in these data as well (see also Eluszkiewicz et al. 1994). The SAO and associated vertical motions are believed to play a role in producing features like the double-peak structures in pressure–latitude cross sections from the Stratospheric and Mesospheric Sounder (SAMS) N_2O and CH_4 fields (Gray and Pyle 1987; Choi and Holton 1991). In the upper stratosphere, temperature-dependent ozone destruction cycles play a dominant role, and the 2-hPa MLS plots appear to follow such trends (e.g., spring midlatitude decreases when temperatures are increasing). These and other features related to the annual and semiannual ozone variations are in general agreement with previous analyses by Perliski and London (1989) and Perliski et al. (1989). Further correlative studies would be useful, however, for quantitative conclusions on these variations. Ray et al. (1994) provide a more detailed analysis of SAO, based on MLS data, and comment on the amplitude characteristics versus pressure–latitude.

An interesting tropical feature is the existence of low ozone abundances at 46 hPa from October 1991 to mid-1992. The low equatorial values (Fig. 1) rise sharply during June–July 1992 and level off until September 1993; during this time period, the low ozone feature splits into two somewhat weaker subtropical lows after June of 1992. From late 1993 on, low values are again observed near the equator. Figure 2 further shows that these low ozone values may be linked to upward motion in connection with the quasi-biennial oscillation (QBO). Indeed, the subtropical lows occur during a period of equatorial westerlies (near 20 hPa), a period traditionally associated with enhanced downward motion at the equator, with upwelling in the subtropics as a result of the return arms of the induced circulation (e.g., Gray and Pyle 1989). Lower-stratospheric observations of H_2O from MLS also show variations possibly associated with the QBO in the lower stratosphere (Carr et al. 1994). Observations of the subtropical ozone QBO, as deduced from TOMS data by Bowman (1989), can place constraints on details of the mechanism for the QBO and the spread of related anomalies to other latitudes. We simply note here that the subtropical low MLS ozone values are reasonably symmetric about the equator. Bowman (1989) and Lait et al. (1989) point out that the TOMS analyses show a more symmetric QBO behavior about the equator than previous analyses of ground-based or *Nimbus-4* Backscatter Ultraviolet (BUV) data. However, uplift effects and circulation changes arising from post-Pinatubo aerosol heating would also have to be considered as an explanation for low tropical ozone (Grant et al. 1992, 1994; Kinne et al. 1992; Pitari 1993; Schoeberl et al. 1993).

Subsequent spreading of the aerosol to higher latitudes would also need to be taken into account; SAGE II aerosol data, for example, have provided much information about the poleward dispersal of Mount Pinatubo aerosol, a process itself partly connected to the QBO (Trepte and Hitchman 1992; Trepte et al. 1993). The time constants for lofting (Kinne et al. 1992), and the fairly symmetric nature of the latitudinal cross sections of aerosol extinction measured by Improved SAMS (ISAMS) (Lambert et al. 1993) and CLAES (Mergenthaler et al. 1993) during 1992 would lead us to believe, however, that the MLS-observed splitting of tropical low ozone values into the subtropics is a result of residual circulation effects, possibly tied to the QBO, as opposed to aerosol-induced lofting effects. We examine further in Fig. 4 the variations in equatorial mixing ratio (ΔO_3) with respect to the mean over the 2.5-yr period of MLS observations. This figure shows that the changes mentioned above for 46 hPa are somewhat anticorrelated with changes occurring at 100 hPa. The MLS variations for 100 hPa are to be viewed with caution, given the decreasing sensitivity at that level; future refinements in the retrieval algorithm may change this behavior somewhat. However, one possible suggestion from the anticorrelated behavior in these lower-stratospheric levels is one of oppositely directed vertical motions at the 100- and 46-hPa levels. The nu-

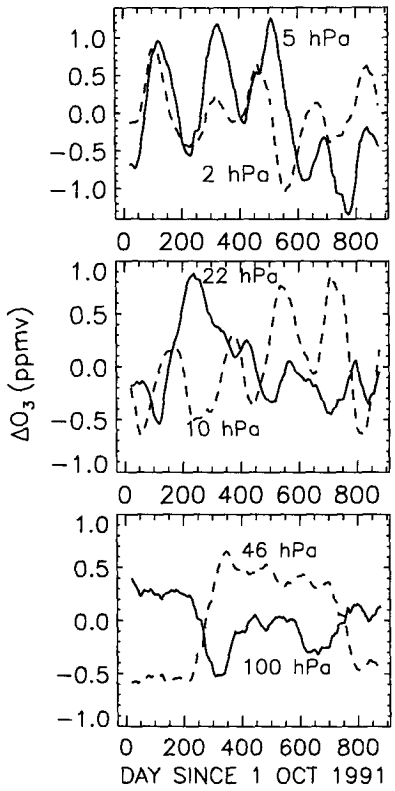

FIG. 4. Equatorial ozone variation (ppmv) about the 2.5-yr mean, as measured by MLS since shortly after launch (time period is same as in Figs. 1 and 2). A 36-day smoothing (running average) has been applied to the data to remove most of the (small) artificial variation coupled to the *UARS* yaw cycle (see text). Panels give mixing ratio changes at various pressures, from 100 to 2 hPa.

merical simulation of the ozone QBO by Gray and Dunkerton (1990) exhibits a 6-month phase shift between the maximum in ozone at altitudes below 23 km and the maximum at about 26 km, which the authors attribute in part to chemical control (NO_y variations) at the higher altitudes; more recent modeling by Chipperfield et al. (1994) leads to a similar result. The observed phase shift between the steep rise in MLS ozone at 22 and 46 hPa appears to agree with that type of behavior. With more MLS data and further analyses, altitude- and latitude-dependent results on the ozone QBO (amplitude and phase) could be obtained, as done for SAGE II data by Zawodny and McCormick (1991). In the middle to upper stratosphere, observed variations displayed in Fig. 4 show a transition toward changes dominated by a semiannual signal (at 10, 5, and 2 hPa), with noticeable phase changes at the different levels.

Pursuing the equatorial variations a little further, we calculate the ozone column by integrating the mixing ratios in the vertical, using the retrieved MLS profile points only (i.e., every other level 3 grid point). Then, based on the MLS level 3AL files, we produce an area-weighted average for the 5°S–5°N bin. In order to study the height dependence in the column amounts, the column ozone values above 100, 46, and 22 hPa are plotted in Fig. 5 as a function of time since 1 October 1991. A 36-day smoothing (running average) has been applied to help remove the known spurious oscillation tied to the UARS "yaw period." While the column above 22 hPa displays a strong semiannual oscillatory behavior, clearly connected to the mixing ratio variations of Fig. 4, the column down to the lower levels (100 and 46 hPa) is also affected by a longer-period variation. We infer that this must be a manifestation of the quasi-biennial oscillation in column ozone (see, e.g., Oltmans and London 1982); a definite characterization of the QBO from MLS data would require a longer time series and removal of the mean annual and semiannual components. More thorough analyses from satellite data have been performed (e.g., Hilsenrath and Schlesinger 1981; Hasebe 1983; Bowman 1989). Nevertheless, it is hoped that further investigation into the 46- and 100-hPa ozone data from MLS (see Fig. 4) will lead to an improved understanding of the QBO signal and its generation. The bottom panel of Fig. 5 shows the zonal-mean winds at the equator, at 46 hPa, and at 22 hPa, based on U. K. Meteorological Office (UKMO) data (Swinbank and O'Neill 1994). The ozone QBO has traditionally been linked to the lower-stratospheric wind QBO and wave-driven vertical motions (Holton and Lindzen 1972; Plumb 1984), which can modulate the total column. Lait et al. (1989) have

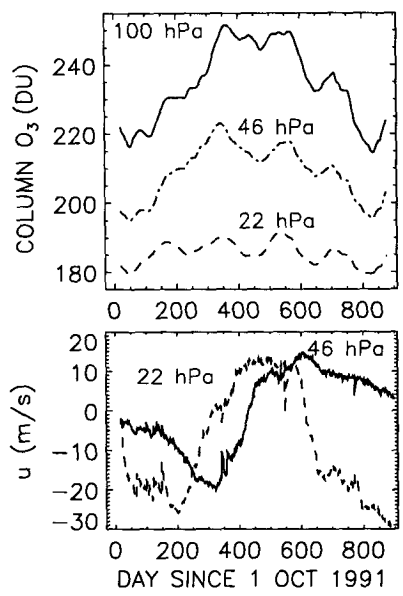

FIG. 5. Top panel: Integrated ozone (DU) from MLS daily data between 5°S and 5°N (area weighted) versus time, for column down to 100 hPa (solid line), 46 hPa (dash–dot line), and 22 hPa (dashed line); note that the latter values have been increased by 50 DU for plotting convenience. Bottom panel: UKMO 1200 UTC zonal-mean winds (m s^{-1}) for same time period, over the equator (solid line for 46 hPa, dashed line for 22 hPa). Positive wind is westerly.

found better correlation between TOMS total column ozone QBO signal and the 30-hPa zonal winds at the equator than with the 50-hPa winds. Also, Bowman (1989) finds maximum correlation between TOMS column ozone data and zonal-mean winds at 20 hPa. This agrees with the general relationship shown in Fig. 5, where better correlation is apparent for winds at pressures of 22 hPa than of 46 hPa. The maximum ozone values occur during the westerly phase of the dynamical QBO near 22 hPa, presumably in connection with the downward motion generally ascribed to this QBO phase (e.g., Hamilton 1989; Gray and Dunkerton 1990). We note that the long-term column ozone variations seen in Fig. 5 (for the columns down to 100 and 46 hPa) are mostly driven by the changes at 46 hPa shown in Fig. 4, in qualitative agreement with the implications from Gray and Dunkerton (1990). Furthermore, the exact phase relationship between ozone- and zonal-mean winds at various heights can be affected by the feedback mechanism of ozone heating on the circulation, as well as by photochemical effects [see the recent work by Hasebe (1994) and earlier modeling by Ling and London (1986)]. Further comparisons with such models would be of much interest, despite the relatively short time span of MLS observations.

We now extend the consideration of column ozone variations to other latitudes, given the importance of the column to attenuation of solar UV radiation and the existence of long-term measurements of column ozone from other instruments.

4. An overview of MLS ozone column data

An analog to the mixing ratio time series of Fig. 1 is shown in Fig. 6, for ozone integrated above 100 hPa, every 16° in latitude. The interannual ozone column changes for this 2.5-yr time period are seen to maximize in the northern midlatitudes. In particular, the 48°N October values are very similar for the three years, but the rate of increase toward the well-known March maximum varies substantially in each of these years. The second year (solid, dark-blue line) shows lower values than the first year (dotted, light-blue line) in the winter, while the third year (thick red line) exhibits ozone values higher than the first year in that season. It turns out that most of these changes are driven by interannual variations in the 100-hPa mixing ratios, as discussed further below. The July–September column ozone values are quite similar during 1992 and 1993 for middle to high northern latitudes. The equatorial column behavior mirrors the changes seen in Fig. 1 at 46 hPa, as shown also in the previous section. Interannual variations at the southernmost latitudes (80°S) are most apparent during the vortex breakup phase (November), as one might expect, and are quite small at other times.

In order to get a broader view of the changes at different latitudes, we have produced area-weighted integrals of the column ozone variations for different latitude bands in Fig. 7 (top left panel), as opposed to the specific latitudes of Fig. 6. The globe has been split into latitude intervals ranging from 0° to 15°, 15° to 30°, 30° to 60° (midlatitudes), and 60° to 80° (polar latitudes); also the 30°S–80°N, 30°S–30°N, and 30°N–80°S bins are shown. The vertical intervals are the same (100 DU from minimum to maximum) except for the 60°–80°S bin. Furthermore, Fig. 7 includes three other panels to give column amounts above 22 hPa, between 100 and 46 hPa, and between 46 and 22 hPa. Again, the striking feature is the northern midlatitude (30°–60°N) wintertime column decrease (or slower rate of increase) during 1992/93 versus 1991/92; an average drop of about 8% (20–25 DU) is evident from mid-December to mid-March (if one assumes continuity in the time interval during which MLS is not viewing these regions). Roughly half of this decrease arises from the layer between 100 and 46 hPa, and another quarter comes from the 46- to 22-hPa layer, as can be seen from an examination of the other

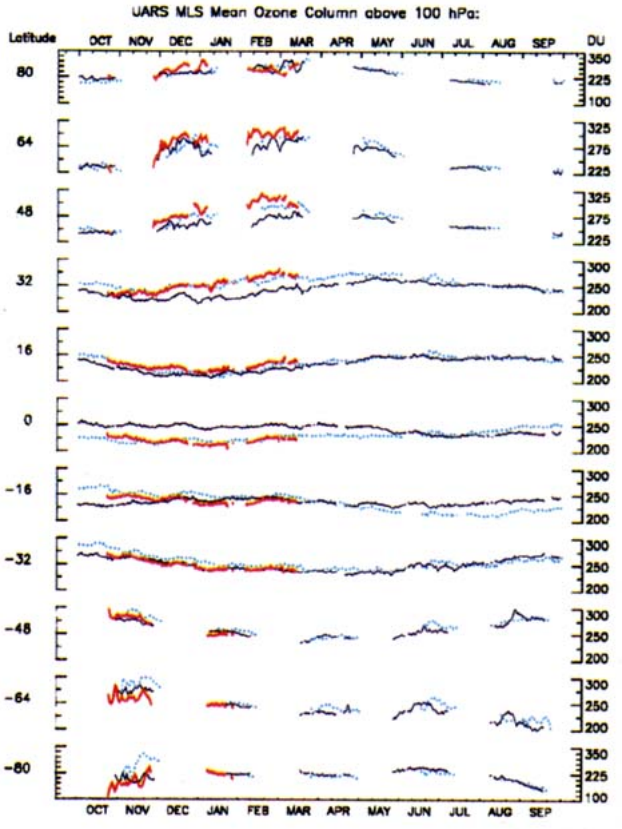

FIG. 6. Time series of MLS zonal-mean ozone column (DU) above 100 hPa, for a time period identical to that of Fig. 1 (October 1991 through mid-March 1994) and for the same 16° increments in latitude. Three curves are shown for each year of data (same identification as in Fig. 1). Vertical scales cover a range of 100 DU for all latitudes except for 80° and −80°, where the variations over a year are larger, particularly in the south.

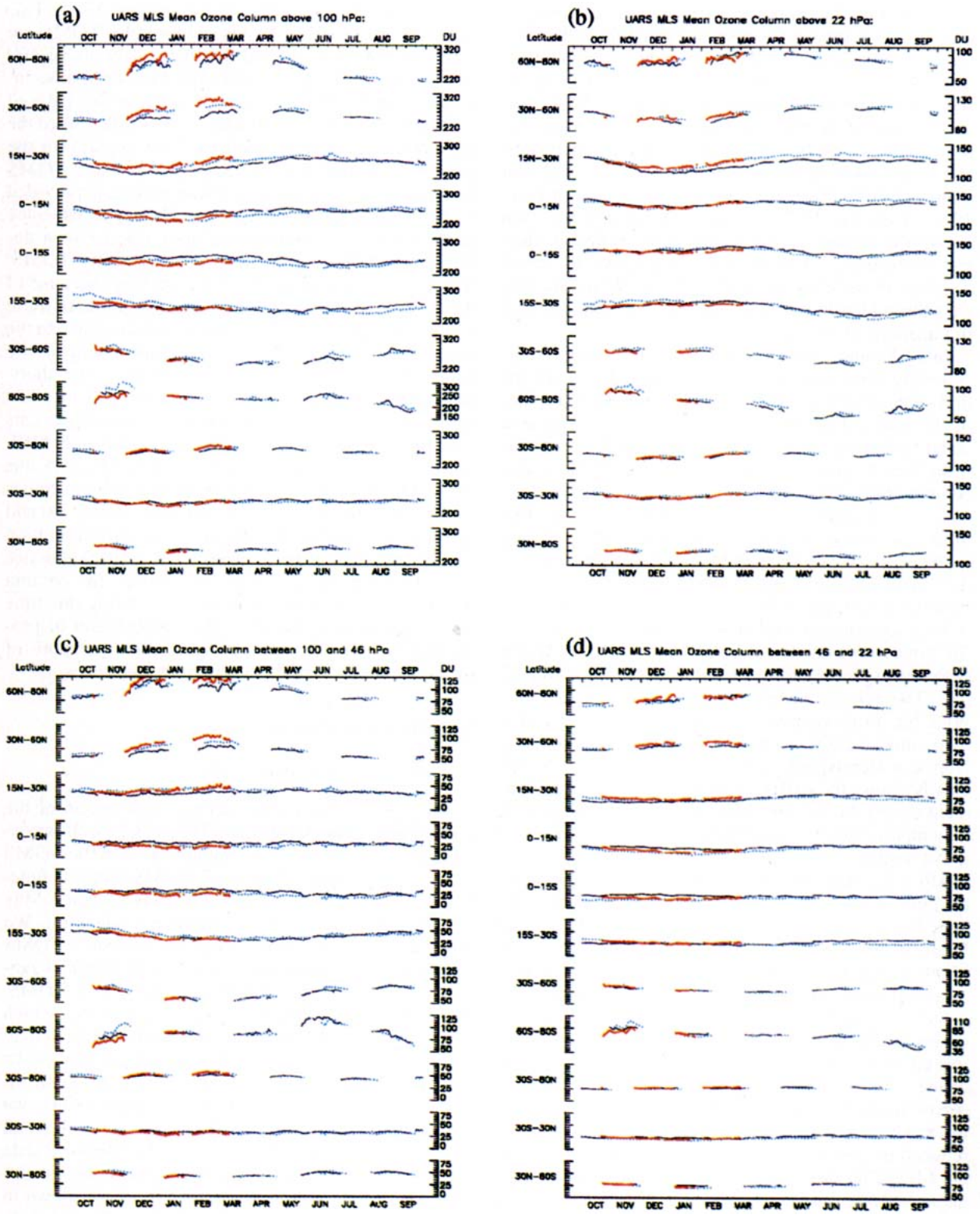

FIG. 7. Area-weighted average MLS ozone column for various latitude bins (see labels), as a function of time since October 1991 (curves have same identification as in Figs. 1 and 6). Mean columns are computed as follows: (a) above 100 hPa, (b) above 22 hPa, (c) between 100 and 46 hPa, and (d) between 46 and 22 hPa.

panels in Fig. 7. Similarly, more than half of the recovery in the 1993/94 winter is coming from the lowermost layer measured here (roughly 50–100 hPa). The 1993 decrease is reduced in May and has essentially disappeared by midsummer. In early 1994, column ozone at northern midlatitudes is roughly 5% higher than in early 1992. The highest northern latitudes also show larger ozone values in late 1993, but values close to the early 1992 measurements in early 1994. While the 1992/93 changes in the 60°–80°N bin are similar to those occurring in the 30°–60°N bin, they are, interestingly, smaller in magnitude; overall, this is also true of the changes in the 15°–30°N bin. We discuss the midlatitude ozone observations and potential implications at greater length in section 5.

In the Tropics, the second year of MLS observations generally shows larger ozone column values than the first year, in contrast to the behavior at higher latitudes in the north. The integral over 30°S–30°N (an area equal to half the global area) shows very little change from year to year and within each year in the ozone column above 100 hPa.

The other fairly large difference of note is the October–November 1992 low ozone in the 15°–30°S bin; in this case, an examination of the mixing ratios shows that these changes appear to come mostly from the pressure levels above 100 hPa (46 hPa in particular). A large component (about half or more) of the 15°–30° bin column ozone values and annual variations (in both hemispheres) comes from the column above 22 hPa. The average ozone column changes in the 30°–60°S bin from year to year are significantly smaller than the average decrease in the corresponding Northern Hemisphere bin. Finally, the 60°–80°S bin clearly shows the existence of an ozone hole development during August and September, and the largest interannual variability is observed during vortex breakup in November.

More focused descriptions of the ozone changes in the polar vortices as observed from MLS data analyses have been given by Waters et al. (1993a, 1993b) and Manney et al. (1993, 1994a, 1994b). In particular, Manney et al. (1994a) discuss the evidence for vortex-averaged ozone depletion in the northern winter, by contrasting the behavior of ozone with long-lived tracers measured by CLAES. Although we see no evidence for an ozone hole development in the zonal-mean ozone column during the winter at 60°–80°N, as observed in the 60°–80°S bin during September, we believe that the rate of increase in the column is no doubt reduced by chlorine-induced ozone destruction (given the MLS ClO observations also presented in some of the above references).

We conclude this section with a comparison of the MLS ozone variations at high southern latitudes with *Nimbus-7* TOMS total column data. Figure 8 gives a height-dependent view of the column changes as seen by MLS, for column above 100, 46, and 22 hPa, during the months of June through November 1992. This shows that the overall trends observed by TOMS are well reproduced in the MLS column data above 100 hPa, both during the decline and the springtime increase. The lack of polar night data in the case of TOMS weights the early winter TOMS data toward the lower latitudes, and accounts (at least in part) for the poorer correlation between average MLS and TOMS columns in July; the more poleward coverage provided by MLS gives an ozone decrease already in late June in the lowermost stratosphere, thus leading to a decrease in column earlier than observable by TOMS. Exact correlation is not expected anyway, because of the different horizontal and vertical resolution of these instruments (TOMS can sample essentially down to the ground, if the effects of clouds and tropospheric profile assumptions on the retrievals are small). The short-term peaks occurring in September are well matched in both datasets; these peaks are tied to warming events (see Fishbein et al. 1993). The figure also adds MLS information on column above other levels, and this shows that most of the depletion in total column comes from a reduction in the ozone amount between 100 and 50 hPa, in agreement with previous finer-resolution vertical profiles from ozonesondes over Antarctica (e.g., Hofmann et al. 1989). In contrast, the column above 22 hPa is observed to increase during this time period, presumably because of a combination of production increase (more sunlight) and transport of ozone from lower latitudes and higher altitudes.

5. Midlatitude ozone decreases

a. Further observational analyses

We pursue here a more detailed description of the midlatitude ozone decreases in 1992/93, as well as possible implications. First, a comparison with the TOMS results is warranted. *Nimbus-7* TOMS stopped functioning in May 1993 (last good full day of data is May 6), after over 14 years of outstanding operation. We have added recent results from the *Meteor-3* TOMS instrument as comparison for 1993, including the 1 January–6 May overlap period with *Nimbus-7* TOMS. The *Meteor-3* instrument is in a precessing orbit, which leads to periods of time during which observations over a good portion of a hemisphere are not possible (solar zenith angles are too high); because of this (and instrument malfunction during most of June 1993), we have omitted all of June at all latitudes, as well as all of July for southern latitudes from the *Meteor-3* data record. The TOMS and MLS column amounts from 1 October 1991 to end of September 1993 are shown in Fig. 9, for the 30°–60° northern and southern latitude regions. We see from the figure that very good agreement is obtained between both TOMS instruments during the 1993 overlap period shown here. The 1992/93 decrease in ozone column is evident in TOMS data (as

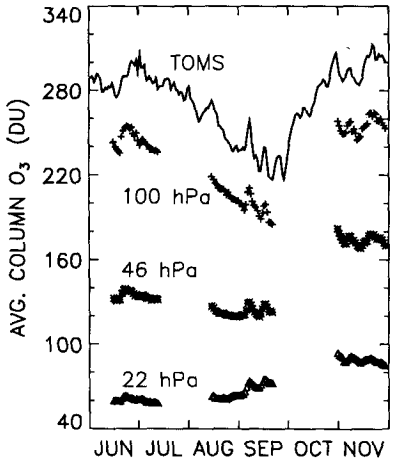

FIG. 8. Column ozone (DU) from *Nimbus-7* TOMS (solid line) and MLS for the 60°–80°S bin, for a time period covering the ozone hole development during the summer and spring of 1992. The various MLS data points are labeled with the pressure down to which the column is computed (TOMS measurements go down to the ground, in principle, which accounts for the larger values).

discussed by Gleason et al. 1993). This is particularly true during winter and spring in the north. Decreases in the south are largest in the early part of the diagram, that is, in October and November. By end of August 1993, TOMS average ozone column amounts have basically recovered to the 1992 values, but may still lie somewhat below the expected lows based on long-term variability (Herman and Larko 1994); these authors note that the average symmetry between hemispheric (long term) decreases has been broken since the onset of large ozone losses in 1992, mostly in the Northern Hemisphere. The MLS ozone column data appear to agree qualitatively with the general results seen by the TOMS instruments over this time period. Large Northern Hemisphere decreases are also seen by MLS, especially in the wintertime, when the absolute decrease is similar in both datasets (20–25 DU). Recovery to 1992 values appears to occur somewhat quicker in the MLS results than in the TOMS data. The recovery in the south (in August) is observed in both datasets. The main difference is in the magnitude of the southern decreases; TOMS-inferred decreases are significantly (50%–100%) larger than the MLS column differences during November and January/February in particular. Keeping in mind the MLS column precision estimates in section 2, and the fact that a large number of profiles (more than 250) are averaged in the latitude bands discussed here, noise in the MLS averages should be at the sub–Dobson unit level. Systematic effects (see also section 2) can remain, as seen, for example, in the artificial oscillations for MLS data within each *UARS* yaw period. These effects (of order 5 DU) are reproduced in both years, however, and should not affect the interannual differences at the systematic levels (more than 10 DU) observed by TOMS in the south. Rather, a systematic interhemispheric difference between both years would have to be invoked, in either TOMS or MLS data. Taken at face value, the differences could imply that the column ozone decreases in the Southern Hemisphere occurred at relatively lower altitudes (with respect to the 100-hPa pressure level) than in the Northern Hemisphere, so that MLS did not quite sample the whole effect in the south. It appears unlikely that aerosol or tropopause height effects could cause such differences in the retrievals between TOMS and MLS measurements, and further investigation into these interhemispheric differences is needed. Unfortunately, there are fewer ground-based or ozonesonde datasets in the south than in the north to help in this matter.

We offer a finer-resolution picture of the MLS column changes in Fig. 10, where the complete zonal-mean column dataset is mapped as a function of time, for the two years discussed above. The bottom panel gives the difference (second year minus the first) and puts the temporal and latitudinal extent of the changes at northern midlatitudes during the first part of the time period (wintertime in particular) in evidence. One of the changes contributing to the observed midlatitude year-to-year differences can be found by examining the

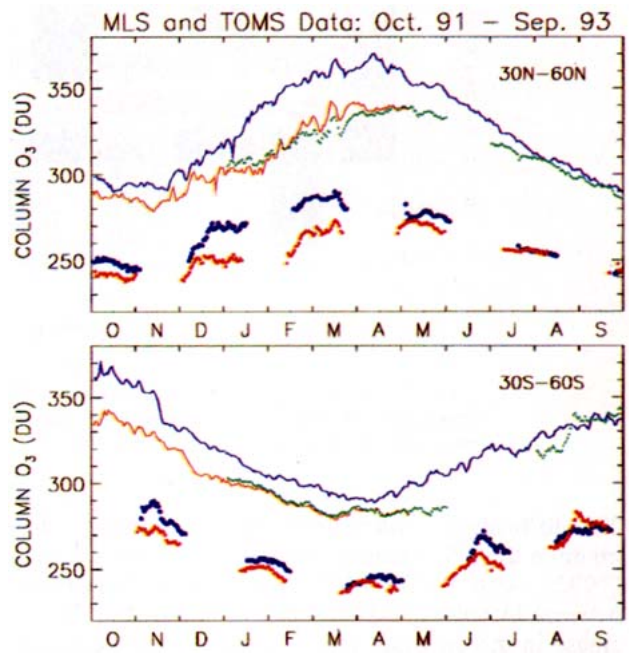

FIG. 9. Column ozone (DU) from TOMS and MLS measurements for the 30°–60°N bin (top panel) and for 30°–60°S (bottom panel), during the October 1991–September 1993 period. *Nimbus-7* TOMS data are the solid lines (blue for 1991/92, red for the lower values of 1992/93). *Meteor-3* TOMS data are shown by dotted green line, overlapping the *Nimbus-7* TOMS results during the 1 January 1993–6 May 1993 interval. MLS column ozone above 100 hPa is shown as blue dots for 1991/92 and as red dots for 1992/93.

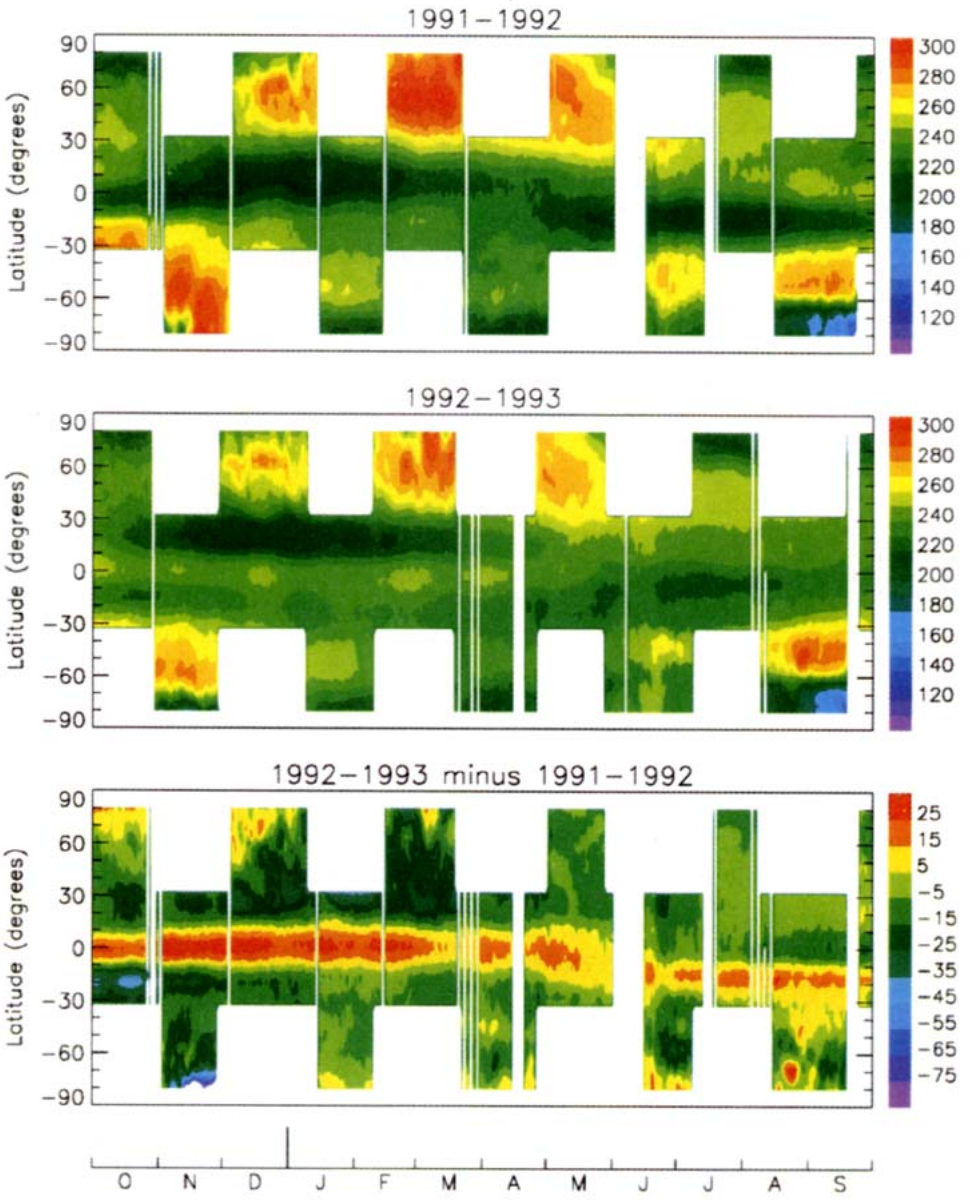

FIG. 10. MLS column ozone time series as a function of latitude for the period 1 October 1991–30 September 1992 (top panel), along with the following year (middle panel) and the difference (second year minus the first, bottom panel). Column values are computed above 100 hPa, in Dobson units (DU).

20°–30°N region, where the depth of the annual minimum in the fall is seen to be larger in the second year (1992). Also, the 30°–40°N band exhibits a decrease between October and December, as opposed to the increase in the previous year. The low ozone values in the 20°–40°N region appear to arise as a combination of the low values at 46 hPa, observed in the splitting of the equatorial low mentioned in section 2, and the overall lower ozone values in the 100-hPa region (see Fig. 2).

Panels in Fig. 11 depict the changes in latitude–pressure cross sections from early December through mid-March, in roughly two-week averages. The first year (1991/92), second year (1992/93), and differences between the two are shown. Ozone concentration (units of 10^{18} molecules per cubic meter), rather than mixing ratio, is plotted to emphasize the lower stratosphere, where changes at 46 and 100 hPa are most important for column abundances. Higher equatorial ozone values are observed near 46 hPa in the second year, as seen clearly in the difference plots, and the early December southern subtropical decrease is also seen. The effect of lower ozone concentrations in the 100-hPa pressure range in particular is evident at midlatitudes, with the

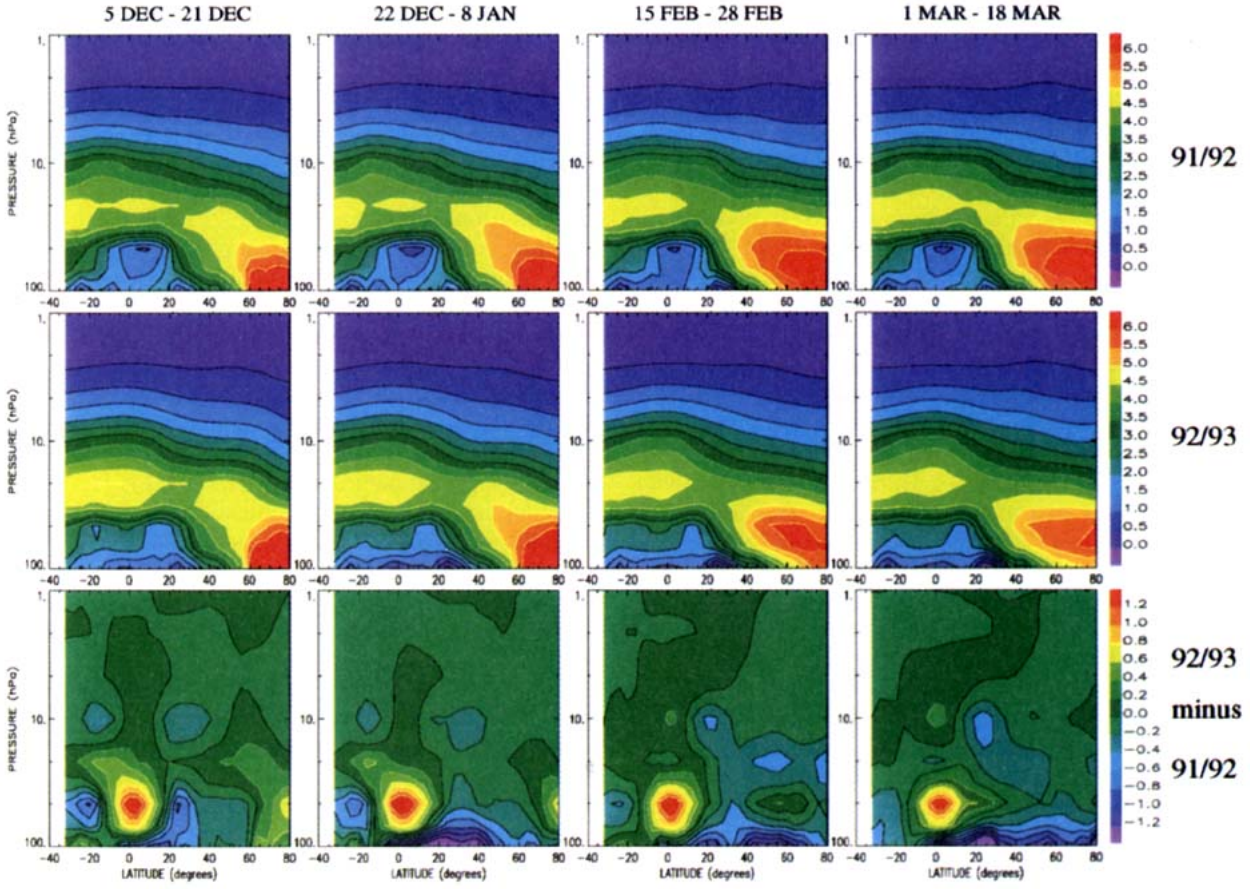

FIG. 11. Time evolution of the latitude–pressure cross section for ozone density (from MLS data, coupled with MLS and NMC temperatures), for roughly two-week averages in the 1991/92 Northern Hemisphere winter (top four panels), 1992/93 winter (middle four panels), as well as the difference (second year minus the first, bottom four panels). Exact days used in averages are indicated above each column; density units are 10^{18} molecules per cubic meter.

differences migrating to higher latitudes as time progresses. In late February and early March, the ozone decreases are spread over a larger vertical extent than during December, possibly as a result of polar vortex processing and subsequent dilution effects at lower latitudes.

b. *Discussion*

Figure 11 is consistent with the long-held views that high-latitude winter–spring ozone column values arise from the poleward and downward transport of large ozone concentrations produced in the Tropics. The midlatitude fall–winter decrease may be related in part to the mixing of lower than usual values from the 50–100-hPa vertical range at low latitudes (20°–40°N) into the lowermost (100 hPa) midlatitude regions. Polar region decreases may have played a role in February and March [indeed, higher ClO is observed by MLS in the vortex in 1993 (Manney et al. 1994a)], but not in the early winter, when high-latitude changes between the two years are small and much lower ClO is present in the vortex. Indeed, MLS results from the previous section show that the ozone decrease in 1992/93 does not start in the polar regions and spread to lower latitudes.

The low ozone values observed at midlatitudes by MLS are generally consistent with other recently reported measurements such as the *Nimbus-7* TOMS results (Gleason et al. 1993), indicating unprecedented low global ozone in 1992; the TOMS update by Herman and Larko (1994), with *Meteor-3* TOMS data added up to July 1993; and other ground-based and satellite results (Bojkov et al. 1993; Kerr et al. 1993; Hofmann et al. 1993; Hofman et al. 1994; Komhyr et al. 1994; Planet et al. 1994). Given the TOMS historical record and statistical models that can fit this record up to 1991, the 1992 and 1993 ozone column changes at northern midlatitudes in particular are significantly outside expectations (Gleason et al. 1993; Herman and Larko 1994). Despite some difference in the magnitude of the hemispheric asymmetry in the decreases dis-

cussed above for MLS versus TOMS, the MLS data support the statements by Herman and Larko (1994) that "there is no longer an average symmetry between the hemispheres," based on the 1992/93 data and comparisons to long-term records (Stolarski et al. 1991, 1992; Herman et al. 1993; McCormick et al. 1992; Niu et al. 1992). The 1994 MLS data appear to show a return to pre-1992 values, which should be more in line with the historical envelope discussed in TOMS data analyses such as those of Herman and Larko (1994). The northern midlatitude ozone decreases observed during the two years after the eruption of Mount Pinatubo (June 1991) are about an order of magnitude larger than the already significant long-term decreases discussed in some of the above references. There were also equatorial ozone decreases (Grant et al. 1992, 1994; Schoeberl et al. 1993; Herman and Larko 1994) in the months just after the eruption. The low MLS equatorial values (late 1991 and early 1992) appear to support the latter findings, but the MLS data lack the long-term record for comparisons from the pre- and post-Pinatubo time periods.

The combination of these observed ozone decreases, as well as the recovery in late 1993, point to Mount Pinatubo as a likely culprit for at least part of the ozone changes. As mentioned above, as well as by Herman and Larko (1994), the timing of the decreases does not support a polar processing/dilution effect alone. Furthermore, known natural causes of ozone decrease such as solar flux variations or QBO effects appear to be too small to explain, by themselves, the large recent changes in ozone (Chandra 1993; Gleason et al. 1993; Herman et al. 1993; Schoeberl et al. 1993). Rather, a combination of effects is probably required, but the timing, duration, magnitude, and latitudinal extent of the ozone decrease all need to be addressed. Heating by the volcanic aerosol appears to have occurred after the Mount Pinatubo eruption (Labitzke and McCormick 1992). Such heating can then lead to uplift (and subsequent adiabatic cooling) in the tropical lower stratosphere (Kinne et al. 1992), with accompanied reductions in the ozone concentration. Further changes in the circulation can also be expected, and some models have addressed these issues (Brasseur and Granier 1992; Granier and Brasseur 1992; Pitari 1993; Pitari and Rizi 1993; Kinnison et al. 1994), even though a fully coupled three-dimensional simulation of the radiative, dynamical, and chemical effects (with realistic aerosol distribution and decay) is a difficult task. Radiative effects alone, however, would lead to a decrease in the tropical ozone amounts, but an increase in the middle to high latitudes (based on such models). Thus, increased chemical destruction associated with heterogeneous reactions on the sulphate aerosols appears to be needed to explain the midlatitude ozone losses. Such effects were discussed previously (Hofmann and Solomon 1989) in connection with the El Chichón eruption, and related observational evidence of post–El Chichón lower-stratospheric ozone decreases has been presented recently by Wen and Frederick (1994). N_2O_5 hydrolysis on sulphate aerosols, and the related decrease in available NO_x and increase in ClO_x (and HO_x), has been implicated as a major reason for long-term trends in ozone (Rodriguez et al. 1991), as well as for observed changes in lower-stratospheric species concentrations (Johnston et al. 1992; Fahey et al. 1993; Avallone et al. 1993; Solomon et al. 1993; Kawa et al. 1993; Coffey and Mankin 1993; Koike et al. 1993, 1994; Webster et al. 1994; Rinsland et al. 1994); aerosol-induced changes in photolysis rates can also cause perturbations in chemical species abundances (e.g., Michelangeli et al. 1989; Michelangeli et al. 1992). However, the early reduction in the Tropics is likely a result of changes in the atmospheric heating and circulation (e.g., Brasseur and Granier 1992).

Model calculations of the impact of heterogeneous reactions on sulphate aerosol (see also Pitari et al. 1991) generally predict largest ozone decreases at high latitudes. A recent 2D model with more realistic aerosol distribution by Rodriguez et al. (1994) gives a reduction (from a background aerosol case) of about 2%–4% in the 30°–60° region, with a peak at latitudes poleward of 60°. Reasons for the high-latitude peak include the larger availability of inorganic chlorine, the longer replenishment time for ozone, and the slower photodissociation rate of HNO_3 produced from the heterogeneous reactions (see also Hofmann and Solomon 1989). Interestingly, ozone destruction cycles involving enhanced HO_x amounts play a larger role than cycles involving the enhanced ClO_x abundances.

The following aspects of the MLS (and TOMS) observations may be the most challenging to understand in detail: 1) the latitudinal extent of the changes, that is, the observations, do not support a high-latitude maximum decrease generally predicted by models; 2) there exists asymmetry in the decreases about the equator; and 3) there is a large decrease in 1993, occurring later than the year directly following the eruption. Issue 1 may have to do with the model treatment of poleward (and cross vortex) transport of the aerosols and related heterogeneous chemistry effects; we also note that QBO effects have not been "removed" from the MLS dataset presented here. Furthermore, if enhanced chemical destruction is taking place at high latitudes as a result of volcanic aerosol, enhanced poleward transport of ozone from higher tropical altitudes could mask the effect. It is interesting that the long-term ozone trends based on TOMS data, as deduced by Niu et al. (1992), show mostly negative values at high latitudes, but some longitudinal regions of increase as well, during the winter only. Finally, we note that model results have traditionally been presented in terms of total column changes, whereas the MLS column data shown here are for pressures down to a maximum of 100 hPa. Since polar ozone amounts below 100 hPa could be contributing significantly to ozone decreases (more so than at

lower latitudes), some of the apparent differences in latitudinal behavior could arise from the different columns used (for models versus observations). For issue 2 above, it is worth noting that enhanced northward transport is not unexpected (see Pitari and Rizi 1993) after the eruption of Mount Pinatubo. How this north–south asymmetry could lead to a larger decrease in ozone in the northern midlatitudes (as opposed to the high-latitude effect mentioned above) is another issue. Details of the transport in the lowermost stratosphere (and possibly the troposphere) could play a role here. For example, Hou et al. (1991) have shown that effects ranging from planetary waves (see also Leovy et al. 1985) to mesospheric drag and tropospheric forcing (in addition to photochemistry) can influence the lower-stratospheric ozone amounts (and the column ozone); they also discuss the north–south asymmetry in transport (in relation to the asymmetry in the spring column maximum). The aerosol observations from SAGE (McCormick and Veiga 1992; Trepte et al. 1993) have shown that the Mount Pinatubo aerosols spread mostly southward in the first months after the eruption; however, the altitude distribution of the northward and southward components was different, with the northward dispersion occurring at lower altitudes. These lowermost stratospheric altitudes may be the critical difference, based on MLS ozone data in both hemispheres. However, the *UARS* aerosol extinction data from ISAMS and CLAES in 1992 do not show much asymmetry between the two hemispheres (Lambert et al. 1993; Mergenthaler et al. 1993); detailed modeling of heterogeneous chemistry including the latitude-dependent Mt. Pinatubo aerosol dispersion and decay would be useful. Deshler et al. (1993) note that at 41°N the important aerosol surface area (and mass) showed a maximum about six months after the eruption, with a fairly steady behavior through 1992. We add that the midlatitude lower-stratospheric ClO data from MLS show little asymmetry between the hemispheres. Also, in connection with question 3, the MLS ClO data make it difficult to explain the 8% reduction in ozone during the winter of 1992/93 by ClO-related chemistry alone (if we use first-order estimates of the impact of the ClO–dimer, ClO–BrO, and ClO–HO_2 rates on ozone column); this is also true for more complete calculations (including HO_x and other cycles) by Rodriguez et al. (1994), who find a few percent reduction in the column. The latter authors point out that saturation of the N_2O_5 hydrolysis heterogeneous reaction occurs during both years following the eruption, and this—combined with the long time constant for ozone in the lower stratosphere—explains the long steady duration of the chemical destruction. Given the magnitude of the observed changes, we find it likely that other effects played a role as well. Although Rodriguez et al. (1994) note that uncertainties in heterogeneous reaction rates could be invoked, this would not resolve the question of an asymmetry between hemispheres (based on their model). Hofmann et al. (1994) point to the QBO as only a partial possible explanation for the larger decreases in ozone observed in ozonesonde data during 1993. Indeed, the QBO phase change with latitude (see, e.g., Zerefos et al. 1992; Chandra 1993; Kalicharran et al. 1993; Chipperfield et al. 1994) would imply a relative high in midlatitude ozone in early 1992, followed by a relative low in early 1993 (essentially opposite in phasing to the variations shown here at the equator for MLS column ozone). The strength of planetary-scale waves is also coupled to the phase of the QBO (Holton and Tan 1980). Based on the MLS data shown in this paper, the Northern Hemisphere subtropical low ozone column during late 1992, and subsequent mixing to higher latitudes during winter in the lowermost stratosphere, could play a part in the low northern midlatitude ozone values during the 1992/93 winter. If the midlatitude lower-stratospheric ozone values during winter occur largely as a result of transport from higher altitudes in the Tropics, however, less efficient transport in 1992/93 would have to be invoked. Previous models (e.g., Tung and Yang 1988) have addressed seasonal changes in column ozone, particularly at high latitudes, but have not emphasized the seasonal behavior of midlatitude ozone in the lowermost stratosphere.

6. Residual ozone (TOMS minus MLS)

Since the ozone data from TOMS give the total column down to the ground (under the caveats mentioned earlier) and are generally quite consistent with ground-based measurements of total column, one is tempted to subtract stratospheric column ozone values from the TOMS data in order to infer tropospheric ozone. Ozone in the troposphere is a precursor for OH, an important radical that controls the oxidization of various source gases, including methane and hydrogenated chlorofluorocarbons (HCFCs). Using TOMS and SAGE data, Fishman et al. (1990) found that residual (TOMS minus SAGE) ozone was large downwind of Africa in the Tropics and that the abundances maximized during the time of biomass burning (the dry season), between July and October. Similar results were obtained by Cros et al. (1992), from an analysis of the satellite data over Brazzaville, Congo (4°S); tropospheric ozonesonde data from that site appear to agree fairly well with the satellite residual values. Tropospheric ozone column amounts in the latter study range from about 30 to 50 DU, with a peak in late summer. Furthermore, the observed seasonal cycle in tropical total ozone column may be dominated by tropospheric ozone variations (Oltmans 1981; Logan and Kirchhoff 1986; Fishman et al. 1986); the amplitude of the seasonal cycle in the Tropics is typically of order 20 DU, and the ozone maximum at the surface tends to occur about two months earlier than the stratospheric ozone peak, based on limited datasets (Oltmans 1981). There is considerable interest in determining the factors that control tropo-

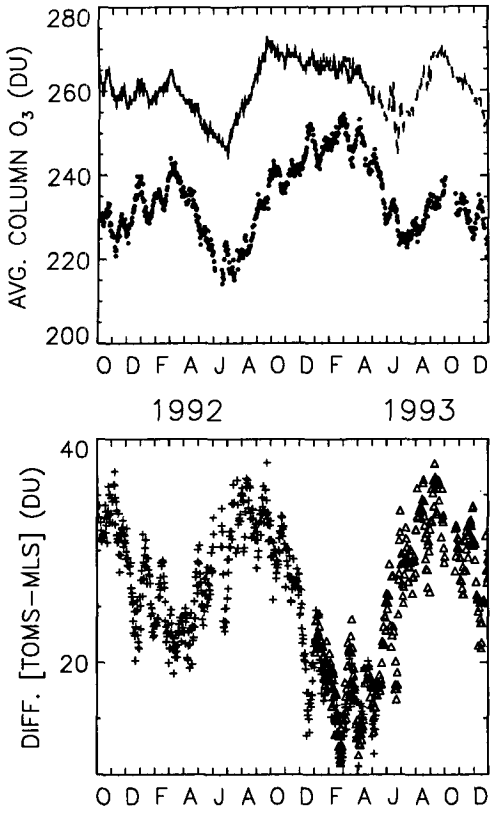

FIG. 12. MLS and TOMS ozone column values for the 5°–10°S bin, during the period 1 October 1991–31 December 1993. Top panel: *Nimbus-7* TOMS total column data are represented as a solid line, *Meteor-3* data as a dashed line (this overlaps the solid line for 1 January 1993–6 May 1993), and MLS column (above 100 hPa) as dots. Bottom panel: Residual difference between the TOMS and MLS column amounts. Plus symbols are for *Nimbus-7* TOMS minus MLS, and triangles are for *Meteor-3* TOMS minus MLS.

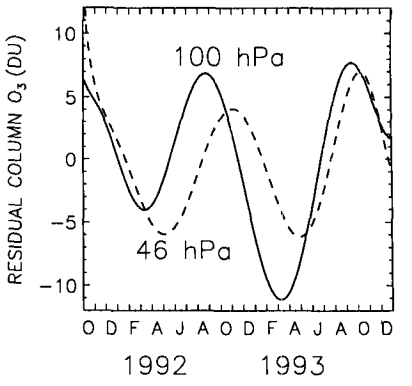

FIG. 13. Residual column amount between TOMS and MLS data for the 5°–10°S bin (same time period as in Fig. 12), for MLS column computed down to 100 hPa (solid line) and down to 46 hPa (dashed line). The lines are polynomial fits through the residual differences (the solid line corresponds to the data shown in the bottom panel of Fig. 12).

spheric ozone; biomass burning and stratospheric intrusions both appear to play an important role (Anderson et al. 1993). The model by Law and Pyle (1993) lends some support to the existence of phase differences between the troposphere and the lower stratosphere in the Tropics.

We show here an example of residual ozone from *Nimbus-7* TOMS minus MLS column ozone (where the MLS column is above 100 hPa). The latitude bin chosen here is 5°–10°S, in a region studied by some of the above authors, because of the existence of heavy biomass burning during July–October. We have looked at several other latitude bins, notably between 30°S and 30°N since the gaps in MLS data at higher latitudes make the analyses somewhat weaker; the 5°–10°S bin gives one of the cleanest residuals (keeping in mind the artificial yaw-period oscillation in MLS data, which can be detected in this figure). The residual ozone has a clear seasonal signature. The amplitude of the variation and the timing of the residual maximum coincide reasonably well with results shown in the above references. It is also interesting that a phase shift is observed between the residual calculated in Fig. 12 and the residual calculated using MLS data down to 46 hPa only (see Fig. 13). This could be interpreted as a phase difference occurring as a result of the different seasonal peaks in the troposphere and stratosphere (since the curve for 46 hPa is more influenced by stratospheric ozone). Preliminary analyses at other latitudes do not yield such a distinct phase change. While these preliminary results may have some significance in terms of tropospheric ozone, we prefer to leave them—in this overview paper—as an indication of potentially interesting signals, which must be interpreted with great care. The existence of MLS systematics at the 5-DU level, along with the interpretation of TOMS data [e.g., in the presence of clouds; see Thompson et al. (1993)], indicate the need for further detailed analyses. An updated version of MLS data, with improvements in the lowermost stratosphere, is planned. Despite caution about the current data and the desire not to make premature statements about "tropospheric ozone" here, we suggest that the MLS dataset, coupled with TOMS ozone column, has the potential for providing valuable information on this interesting topic.

7. Conclusions

We have reviewed the observed variations in MLS stratospheric ozone data, based on analyses of two and a half years (October 1991 to mid-March 1994) of zonal-mean mixing ratios and column abundances. Expected periodic variations are clearly observed; for example, we note the existence of a clear SAO in tropical ozone, for pressures less than about 20 hPa, and a dominant annual cycle at middle to high latitudes. Interesting variations are measured in the tropical lower stratosphere: in particular, a low equatorial ozone feature

near 50 hPa, which splits into two subtropical lows during the summer of 1992 and re-forms a single (equatorial) branch during the fall of 1993. Given the time constants for the maintenance of aerosol lofting effects (Kinne et al. 1992) and the observed dispersal of aerosols, we would tend to ascribe these lower-stratospheric variations to changes in the residual circulation, possibly QBO-related, as opposed to an aerosol-induced, change. MLS ozone column data comparisons with TOMS data in the southern high latitudes (60°–80°S) exhibit seasonal trends (for June–November) consistent with the overall TOMS variations; the ozone hole development is shown to occur primarily as a result of decreases in the 100- to 50-hPa region (in agreement with other data). Based on MLS zonal-mean data, the decrease is primarily driven by changes near 50 hPa. The largest ozone column changes from year to year have occurred during the December to March time frame at northern midlatitudes, with the 1992/93 wintertime values typically 8% lower than the corresponding 1991/92 abundances. This slowing in the rate of ozone increase during the winter months appears to be related in large part to decreases in the lowermost stratosphere (near 100 hPa) during early winter, with an associated poleward spread, rather than a polar effect that migrates south; however, dilution effects from chlorine-related processing of polar ozone may have contributed to the decreases during February and March 1993, based on the significantly enhanced ClO values observed in the Arctic vortex at that time (Manney et al. 1994a). While the phasing of the QBO is expected to lead to low ozone at midlatitudes in late 1992, compared to early 1992, this effect alone would not be expected to be large enough to explain the observations. Since models do not predict that radiative and dynamical changes could, by themselves, lead to the type of midlatitude behavior observed, it is likely that chemical cycles causing ozone destruction as a result of heterogeneous chemistry on volcanic aerosols have played a role in the observed decreases, as predicted by various models. However, the latitudinal extent of the changes (maximum decrease is not at high latitudes) and the asymmetry in the decrease (northern midlatitudes significantly more affected than the southern midlatitudes) are not easy to understand without more detailed modeling. We note also that the TOMS-inferred asymmetry is somewhat less pronounced than the MLS-deduced effect. One mechanism that could, in principle, explain the asymmetry, would be poleward mixing of aerosol and low tropical ozone, with stronger mixing toward the northern winter midlatitudes. A detailed analysis of other chemical species (or dynamical tracers) would be desirable, possibly from the Cryogenic Limb Array Etalon Spectrometer (CLAES) dataset (even though these observations ceased in early summer 1993). An examination of aerosol, HNO_3, and NO_x fields (in addition to the ClO from MLS) may also shed some light on the magnitude of possible changes caused by heterogeneous chemistry.

The low ozone values observed by MLS and other instruments from late 1991 to mid-1993 appear to have essentially disappeared during the late fall 1993 and early winter 1994. This recovery also seems to imply that effects related to the eruption of Mount Pinatubo were involved in the temporary ozone depletion, in combination with QBO and other effects. We expect that future analyses of the MLS data, in conjunction with others from *UARS* and elsewhere, will continue to educate us about the particularly interesting ozone variations that have occurred during the *UARS* mission.

Finally, analyses of the TOMS minus MLS residual ozone column should eventually improve our understanding of tropospheric ozone variations, and this paper's brief presentation of residual ozone gives a preliminary indication of the potential use of these combined datasets.

Acknowledgments. The work of the entire MLS team (hardware, software, and science), along with the *UARS* Project efforts, are gratefully acknowledged for making this dataset possible. In particular, this paper benefited from T. Lungu's efforts on retrieval software and B. P. Ridenoure's able technical support and comments; thanks also go to V. S. Perun and R. P. Thurstans. The data on zonal-mean winds were provided via G. L. Manney and R. W. Zurek, whose comments are also appreciated; the generation of the wind data is thanks to the U. K. Meteorological Office (A. O'Neill and R. Swinbank). Comparisons with TOMS would not have been possible without the generation and availability of the TOMS data, for which we thank the TOMS ozone processing teams at NASA Goddard Space Flight Center. Special thanks to J. F. Gleason for the transfer of data files and valuable comments, as well as J. R. Herman; discussions with R. S. Stolarski and G. Labow were also useful. This research was sponsored by NASA's *Upper Atmosphere Research Satellite* Project and was performed at the Jet Propulsion Laboratory, California Institute of Technology, under contract with the National Aeronautics and Space Administration.

REFERENCES

Anderson, B. E., G. L. Gregory, J. D. W. Barrick, J. E. Collins, G. W. Sachse, C. H. Hudgins, J. D. Bradshaw, and S. T. Sandholm, 1993: Factors influencing dry season ozone distributions over the tropical south Atlantic. *J. Geophys. Res.*, **98,** 23 491–23 500.

Avallone, L. M., D. W. Toohey, M. H. Proffitt, J. J. Margitan, K. R. Chan, and J. G. Anderson, 1993: In situ measurements of ClO at mid-latitudes: Is there an effect from Mt. Pinatubo? *Geophys. Res. Lett.*, **20,** 2519–2522.

Barath, F., and Coauthors, 1993: The Upper Atmosphere Research Satellite Microwave Limb Sounder instrument. *J. Geophys. Res.*, **98,** 10 751–10 762.

Bluth, G. J. S., S. D. Doiron, C. C. Schnetzler, A. J. Krueger, and L. S. Walter, 1992: Global tracking of the SO_2 clouds from the

June, 1991 Mount Pinatubo eruption. *Geophys. Res. Lett.*, **19,** 151–154.

Bojkov, R. D., C. S. Zerefos, D. S. Balis, I. C. Ziomas, and A. F. Bais, 1993: Record low total ozone during northern winters of 1992 and 1993. *Geophys. Res. Lett.*, **20,** 1351–1354.

Bowman, K. P., 1989: Global patterns of the quasi-biennial oscillation in total ozone. *J. Atmos. Sci.*, **46,** 3328–3343.

Brasseur, G. P., and C. Granier, 1992: Mount Pinatubo aerosols, chlorofluorocarbons, and ozone depletion. *Science,* **257,** 1239–1242.

Carr, E. S., and coauthors, 1994: MLS stratospheric water vapour at the tropics. *Geophys. Res. Lett.*, submitted.

Chandra, S., 1993: Changes in stratospheric ozone and temperature due to the eruption of Mt. Pinatubo. *Geophys. Res. Lett.*, **20,** 33–36.

Chipperfield, M. P., L. J. Gray, J. S. Kinnersley, and J. Zawodny, 1994: A two-dimensional model study of the QBO signal in SAGE II NO_2 and O_3. *Geophys. Res. Lett.*, **21,** 589–592.

Choi, W. K., and J. R. Holton, 1991: Transport of N_2O in the stratosphere related to the equatorial semiannual oscillation. *J. Geophys. Res.*, **96,** 22 543–22 557.

Coffey, M. T., and W. G. Mankin, 1993: Observations of the loss of stratospheric NO_2 following volcanic eruptions. *Geophys. Res. Lett.*, **20,** 2873–2876.

Cros, B., D. Nganga, A. Minga, J. Fishman, and V. Brackett, 1992: Distribution of tropospheric ozone at Brazzaville, Congo, determined from ozonesonde measurements. *J. Geophys. Res.*, **97,** 12 869–12 875.

Deshler, T., B. J. Johnson, and W. R. Rozier, 1993: Balloonborne measurements of Pinatubo aerosol during 1991 and 1992 at 41N: Vertical profiles, size distribution, and volatility. *Geophys. Res. Lett.*, **20,** 1435–1438.

Elson, L. S., G. L. Manney, L. Froidevaux, and J. W. Waters, 1994: Large-scale variations in ozone from the first two years of *UARS* MLS data. *J. Atmos. Sci.*, **51,** 2867–2876.

Eluszkiewicz, J., D. Crisp, R. W. Zurek, L. S. Elson, E. F. Fishbein, L. Froidevaux, J. W. Waters, R. S. Harwood, and G. E. Peckham, 1994: Residual circulation in the stratosphere and lower mesosphere as diagnosed from Microwave Limb Sounder data. *J. Atmos. Sci.*, submitted.

Fahey, D. W., and coauthors, 1993: In situ measurements constraining the role of sulphate aerosols in midlatitude ozone depletion. *Nature,* **363,** 509–514.

Fishbein, E. F., L. S. Elson, L. Froidevaux, G. L. Manney, W. G. Read, J. W. Waters, and R. W. Zurek, 1993: MLS observations of stratospheric waves in temperature and O_3 during the 1992 southern winter. *Geophys. Res. Lett.*, **20,** 1255–1258.

Fishman, J., P. Minnis, and H. G. Reichle Jr., 1986: Use of satellite data to study tropospheric ozone in the tropics. *J. Geophys. Res.*, **91,** 14 451–14 465.

——, C. E. Watson, J. C. Larsen, and J. A. Logan, 1990: Distribution of tropospheric ozone determined from satellite data. *J. Geophys. Res.*, **95,** 3599–3617.

Gleason, J. F., and coauthors, 1993: Record low global ozone in 1992. *Science,* **260,** 523–526.

Granier, C., and G. Brasseur, 1992: Impact of heterogeneous chemistry on model predictions of ozone changes. *J. Geophys. Res.*, **97,** 18 015–18 033.

Grant, W. B., J. Fishman, E. V. Browell, V. G. Brackett, D. Nganga, A. Minga, B. Cros, R. E. Veiga, C. F. Butler, M. A. Fenn, and G. D. Nowicki, 1992: Observations of reduced ozone concentrations in the tropical stratosphere after the eruption of Mt. Pinatubo. *Geophys. Res. Lett.*, **19,** 1109–1112.

——, and coauthors, 1994: Aerosol-associated changes in tropical stratospheric ozone following the eruption of Mt. Pinatubo. *J. Geophys. Res.*, **99,** 8197–8211.

Gray, L. J., and J. A. Pyle, 1987: Two-dimensional model studies of equatorial dynamics and tracer distributions. *Quart. J. Roy. Meteor. Soc.*, **113,** 635–651.

——, and ——, 1989: A two-dimensional model of the quasi-biennial oscillation of ozone. *J. Atmos. Sci.*, **46,** 203–220.

——, and T. J. Dunkerton, 1990: The role of the seasonal cycle in the quasi-biennial oscillation of ozone. *J. Atmos. Sci.*, **47,** 2429–2451.

Hamilton, K., 1989: Interhemispheric asymmetry and annual synchronization of the ozone quasi-biennial oscillation. *J. Atmos. Sci.*, **46,** 1019–1025.

Harwood, R. S., and coauthors, 1993: Springtime stratospheric water vapour in the Southern Hemisphere as measured by MLS. *Geophys. Res. Lett.*, **20,** 1235–1238.

Hasebe, F., 1983: Interannual variations of global total ozone revealed from Nimbus 4 BUV and ground-based observations. *J. Geophys. Res.*, **88,** 6819–6834.

——, 1994: Quasi-biennial oscillations of ozone and diabatic circulation in the equatorial stratosphere. *J. Atmos. Sci.*, **51,** 729–745.

Herman, J. R., and D. Larko, 1994: Low ozone amounts during 1992–93 from Nimbus 7 and Meteor 3 Total Ozone Mapping Spectrometers. *J. Geophys. Res.*, **99,** 3483–3496.

——, R. McPeters, and D. Larko, 1993: Ozone depletion at northern and southern latitudes derived from January 1979 to December 1991 Total Ozone Mapping Spectrometer data. *J. Geophys. Res.*, **98,** 12 783–12 793.

Hilsenrath, E., and B. M. Schlesinger, 1981: Total ozone seasonal and interannual variations derived from the 7 year Nimbus-4 BUV data set. *J. Geophys. Res.*, **86,** 12 087–12 096.

Hofmann, D. J., and S. Solomon, 1989: Ozone destruction through heterogeneous chemistry following the eruption of El Chichón. *J. Geophys. Res.*, **94,** 5029–5041.

——, J. W. Harder, J. M. Rosen, J. V. Hereford, and J. R. Carpenter, 1989: Ozone profile measurements at McMurdo station, Antarctica, during the spring of 1987. *J. Geophys. Res.*, **94,** 16 527–16 536.

——, S. J. Oltmans, J. M. Harriss, W. D. Komhyr, J. A. Lathrop, T. DeFoor, and D. Kuniyuki, 1993: Ozonesonde measurements at Hilo, Hawaii following the eruption of Pinatubo. *Geophys. Res. Lett.*, **20,** 1555–1558.

——, ——, W. D. Komhyr, J. M. Harriss, J. A. Lathrop, A. O. Langford, T. Deshler, B. J. Johnson, A. Torres, and W. A. Matthews, 1994: Ozone loss in the lower stratosphere over the United States in 1992–93: Evidence for heterogeneous chemistry on the Pinatubo aerosol. *Geophys. Res. Lett.*, **21,** 65–68.

Holton, J. R., and R. S. Lindzen, 1972: An updated theory for the quasi-biennial cycle of the tropical stratosphere. *J. Atmos. Sci.*, **29,** 1076–1080.

——, and H.-C. Tan, 1980: The influence of the equatorial quasi-biennial oscillation on the global circulation at 50 mb. *J. Atmos. Sci.*, **37,** 2200–2208.

Hou, A. Y., H. R. Schneider, and M. K. W. Ko, 1991: A dynamical explanation for the asymmetry in zonally averaged column abundances of ozone between northern and southern springs. *J. Atmos. Sci.*, **48,** 547–556.

Johnston, P. V., R. L. McKenzie, J. G. Keys, and W. A. Matthews, 1992: Observations of depleted stratospheric NO_2 following the Pinatubo volcanic eruption. *Geophys. Res. Lett.*, **19,** 211–213.

Kalicharran, S., R. D. Diab, and F. Sokolic, 1993: Trends in total ozone over southern African stations between 1979 and 1991. *Geophys. Res. Lett.*, **20,** 2877–2880.

Kawa, S. R., and coauthors, 1993: Interpretation of NO_x/NO_y observations from AASE-II using a model of chemistry along trajectories. *Geophys. Res. Lett.*, **20,** 2507–2510.

Kerr, J. B., D. W. Wardle, and D. W. Tarrasick, 1993: Record low ozone values over Canada in early 1993. *Geophys. Res. Lett.*, **20,** 1979–1982.

Kinne, S., O. B. Toon, and M. J. Prather, 1992: Buffering of stratospheric circulation by changing amounts of tropical ozone. A Pinatubo case study. *Geophys. Res. Lett.*, **19,** 1927–1930.

Kinnison, D. E., K. E. Grant, P. S. Connell, D. J. Wuebbles, and D. A. Rotman, 1994: The chemical and radiative effects of the Mt. Pinatubo eruption. *J. Geophys. Res.*, submitted.

Koike, M. Y., Y. Kondo, W. A. Matthews, P. V. Johnston, and K. Yamazaki, 1993: Decrease of stratospheric NO_2 at 44N caused

by Pinatubo volcanic aerosols. *Geophys. Res. Lett.*, **20,** 1975–1978.

——, N. B. Jones, W. A. Matthews, P. V. Johnston, R. L. McKenzie, D. Kinnison, and J. Rodriguez, 1994: Impact of Pinatubo aerosols on the partitioning between NO_2 and HNO_3. *Geophys. Res. Lett.*, **21,** 597–600.

Komhyr, W. D., R. D. Grass, R. D. Evans, R. K. Leonard, and D. M. Quincy, 1994: Unprecedented 1993 ozone decrease over the United States from Dobson spectrophotometer observations. *Geophys. Res. Lett.*, **21,** 201–204.

Labitzke, K., and M. P. McCormick, 1992: Stratospheric temperature increases due to Pinatubo aerosols. *Geophys. Res. Lett.*, **19,** 207–210.

Lait, L. R., M. R. Schoeberl, and P. A. Newman, 1989: Quasi-biennial modulation of the Antarctic ozone depletion. *J. Geophys. Res.*, **94,** 11 559–11 571.

Lambert, A., R. G. Grainger, J. J. Remedios, C. D. Rodgers, M. Corney, and F. W. Taylor, 1993: Measurements of the evolution of the Mt. Pinatubo aerosol cloud by ISAMS. *Geophys. Res. Lett.*, **20,** 1287–1290.

Law, K. S., and J. A. Pyle, 1993: Modeling trace gas budgets in the troposphere. 1. Ozone and odd nitrogen. *J. Geophys. Res.*, **98,** 18 377–18 400.

Leovy, C. B., C.-R. Sun, M. H. Hitchman, E. E. Remsberg, J. M. Russell III, L. L. Gordley, J. G. Gille, and L. V. Lyjak, 1985: Transport of ozone in the middle stratosphere: Evidence for planetary wave breaking. *J. Atmos. Sci.*, **42,** 230–244.

Ling, X-D., and J. London, 1986: The quasi-biennial oscillation of ozone in the tropical middle stratosphere: A one-dimensional model. *J. Atmos. Sci.*, **43,** 3122–3137.

Logan, J. A., and V. W. J. H. Kirchhoff, 1986: Seasonal variations of tropospheric ozone at Natal, Brazil. *J. Geophys. Res.*, **91,** 7875–7881.

Manney, G. L., L. Froidevaux, J. W. Waters, L. S. Elson, E. F. Fishbein, R. W. Zurek, R. S. Harwood, and W. A. Lahoz, 1993: The evolution of ozone observed by UARS MLS in the 1992 late winter southern polar vortex. *Geophys. Res. Lett.*, **20,** 1279–1282.

——, and Coauthors, 1994a: Chemical depletion of lower stratospheric ozone in the 1992–1993 northern winter vortex. *Nature,* in press.

——, L. Froidevaux, R. W. Zurek, J. W. Waters, A. O'Neill, and R. Swinbank, 1994b: Lagrangian transport calculations using *UARS* data. Part II: Ozone. *J. Atmos. Sci.,* submitted.

McCormick, M. P., and R. E. Veiga, 1992: SAGE II measurements of early Pinatubo aerosols. *Geophys. Res. Lett.*, **19,** 155–158.

——, ——, and W. P. Chu, 1992: Stratospheric ozone profile and total ozone trends derived from the SAGE I and SAGE II data. *Geophys. Res. Lett.*, **19,** 269–272.

——, L. W. Thomason, and C. R. Trepte, 1994: Atmospheric effects of the Mt. Pinatubo eruption. *Nature,* submitted.

Mergenthaler, J. L., J. B. Kumer, and A. E. Roche, 1993: CLAES south-looking aerosol observations for 1992. *Geophys. Res. Lett.*, **20,** 1295–1298.

Michelangeli, D., M. Allen, and Y. L. Yung, 1989: El Chichón volcanic aerosols: Impact of radiative, thermal and chemical perturbations. *J. Geophys. Res.*, **94,** 18 429–18 443.

——, ——, ——, R.-L. Shia, D. Crisp, and J. Eluszkiewicz, 1992: Enhancement of atmospheric radiation by an aerosol layer. *J. Geophys. Res.*, **97,** 865–874.

Niu, X., J. E. Frederick, M. L. Stein, and G. C. Tiao, 1992: Trends in column ozone based on TOMS data: Dependence on month, latitude, and longitude. *J. Geophys. Res.*, **97,** 14 661–14 669.

Oltmans, S. J., 1981: Surface ozone measurements in clean air. *J. Geophys. Res.*, **86,** 1174–1180.

——, and J. London, 1982: The quasi-biennial oscillation in atmospheric ozone. *J. Geophys. Res.*, **87,** 8981–8989.

Perliski, L. M., and J. London, 1989: Satellite observed long-term averaged seasonal and spatial ozone variations in the stratosphere. *Planet. Space Sci.*, **37,** 1509–1525.

——, S. Solomon, and J. London, 1989: On the interpretation of seasonal variations of stratospheric ozone. *Planet. Space Sci.*, **37,** 1527–1538.

Pitari, G., 1993: A numerical study of the possible perturbation of stratospheric dynamics due to Pinatubo aerosols: Implications for tracer transport. *J. Atmos. Sci.*, **50,** 2442–2461.

——, and V. Rizi, 1993: An estimate of the chemical and radiative perturbation of stratospheric ozone following the eruption of Mt. Pinatubo. *J. Atmos. Sci.*, **50,** 3260–3276.

——, G. Visconti, and V. Rizi, 1991: Sensitivity of stratospheric ozone to heterogeneous chemistry on sulfate aerosols. *Geophys. Res. Lett.*, **18,** 833–836.

Planet, W. G., J. H. Lienesch, A. J. Miller, R. Nagatani, R. D. McPeters, E. Hilsenrath, R. P. Cebula, M. T. DeLand, C. G. Wellemeyer, and K. Horvath, 1994: Northern Hemisphere total ozone values from 1989–1993 determined with the NOAA-11 Solar Backscatter Ultraviolet (SBUV/2) instrument. *Geophys. Res. Lett.*, **21,** 205–208.

Plumb, R. A., 1984: The quasi-biennial oscillation. *Dynamics of the Middle Atmosphere,* J. R. Holton and T. Matsuno, Eds., Terra Scientific, 217–251.

Ray, E., J. R. Holton, E. F. Fishbein, L. Froidevaux, and J. W. Waters, 1994: The tropical semiannual oscillation (SAO) in temperature and ozone as observed by the Microwave Limb Sounder (MLS). *J. Atmos. Sci.*, 3045–3052.

Read, W. G., L. Froidevaux, and J. W. Waters, 1993: Microwave Limb Sounder Measurement of stratospheric SO_2 from the Mt. Pinatubo volcano. *Geophys. Res. Lett.*, **20,** 1299–1302.

Reber, C. A., 1993: The Upper Atmosphere Research Satellite. *Geophys. Res. Lett.*, **20,** 1215–1218.

Rinsland, C. P., M. R. Gunson, M. C. Abrams, L. L. Lowes, R. Zander, E. Mahieu, A. Goldman, M. K. W. Ko, J. M. Rodriguez, and N. D. Sze, 1994: Heterogeneous conversion of N_2O_5 to HNO_3 in the post–Mount Pinatubo eruption stratosphere. *J. Geophys. Res.*, **99,** 8213–8219.

Rodgers, C. D., 1976: Retrieval of atmospheric temperature and composition from remote measurements of thermal radiation. *Rev. Geophys. Space Phys.*, **14,** 609–624.

Rodriguez, J. M., M. K. W. Ko, and N. D. Sze, 1991: Role of heterogeneous conversion of N_2O_5 on sulfate aerosols in the global ozone losses. *Nature,* **352,** 134–137.

——, ——, ——, C. W. Heisey, G. K. Yue, and M. P. McCormick, 1994: Ozone response to enhanced heterogeneous processing after the eruption of Mt. Pinatubo. *Geophys. Res. Lett.*, **21,** 209–212.

Schoeberl, M. R., P. K. Barthia, E. Hilsenrath, and O. Torres, 1993: Tropical ozone loss following the eruption of Mt. Pinatubo. *Geophys. Res. Lett.*, **20,** 29–32.

Solomon, S., R. W. Sanders, R. R. Garcia, and J. G. Keys, 1993: Enhanced chlorine dioxide and ozone depletion in Antarctica due to volcanic aerosols. *Nature,* **363,** 245–248.

Stolarski, R. S., P. Bloomfield, R. D. McPeters, and J. R. Herman, 1991: Total ozone trends deduced from Nimbus-7 TOMS data. *Geophys. Res. Lett.*, **18,** 1015–1018.

——, R. Bojkov, L. Bishop, C. Zerefos, J. Staehelin, and J. Zawodny, 1992: Measured trends in stratospheric ozone. *Science,* **256,** 342–349.

Swinbank, R., and A. O'Neill, 1994: A stratosphere–troposphere data assimilation system. *Mon. Wea. Rev.*, **122,** 686–702.

Thompson, A. M., D. P. McNamara, K. E. Pickering, and R. D. McPeters, 1993: Effect of marine stratocumulus on TOMS ozone. *J. Geophys. Res.*, **98,** 23 051–23 057.

Trepte, C. R., and M. H. Hitchman, 1992: The stratospheric tropical circulation deduced from satellite aerosol data. *Nature,* **355,** 626–628.

——, R. E. Veiga, and M. P. McCormick, 1993: The poleward dispersal of Mount Pinatubo volcanic aerosol. *J. Geophys. Res.*, **98,** 18 562–18 573.

Tung, K. K., and H. Yang, 1988: Dynamical component of seasonal and year-to-year changes in Antarctic and global ozone. *J. Geophys. Res.*, **93,** 12 537–12 559.

Waters, J. W., 1993: Microwave limb sounding. *Atmospheric Remote Sensing by Microwave Radiometry,* M. A. Janssen, Ed., John Wiley & Sons, 383–496.

——, L. Froidevaux, W. G. Read, G. L. Manney, L. S. Elson, D. A. Flower, R. F. Jarnot, and R. S. Harwood, 1993a: Stratospheric ClO and ozone from the Microwave Limb Sounder on the Upper Atmosphere Research Satellite. *Nature,* **362,** 597–602.

——, ——, G. L. Manney, W. G. Read, L. S. Elson, 1993b: MLS observations of lower stratospheric ClO and O_3 in the 1992 Southern Hemisphere winter. *Geophys. Res. Lett.,* **20,** 1219–1222.

Webster, C. R., R. D. May, M. Allen, L. Jaeglé, and M. P. McCormick, 1994: Balloon profiles of stratospheric NO_2 and HNO_3 for testing the heterogeneous hydrolysis of N_2O_5 on sulfate aerosols. *Geophys. Res. Lett.,* **21,** 53–56.

Wen, G., and J. E. Frederick, 1994: Ozone within the El Chichón aerosol cloud inferred from solar backscatter ultraviolet continuous-scan measurements. *J. Geophys. Res.,* **99,** 1263–1271.

Zawodny, J. M., and M. P. McCormick, 1991: Stratospheric aerosol and gas experiment II measurements of the quasi-biennial oscillation of ozone and nitrogen dioxide. *J. Geophys. Res.,* **96,** 9371–9377.

Zerefos, C. S., A. F. Bais, I. C. Ziomas, and R. D. Bojkov, 1992: On the relative importance of quasi-biennial oscillation and El Niño/Southern Oscillation in the revised Dobson total ozone records. *J. Geophys. Res.,* **97,** 10 135–10 144.